

AD-A056 894

MISSISSIPPI UNIV UNIVERSITY DEPT OF ELECTRICAL ENGIN--ETC F/G 9/5
CHARGE CONDITION AT THE JUNCTION OF UNEQUAL RADII WIRES. PART I--ETC(U).
FEB 78 B M DUFF

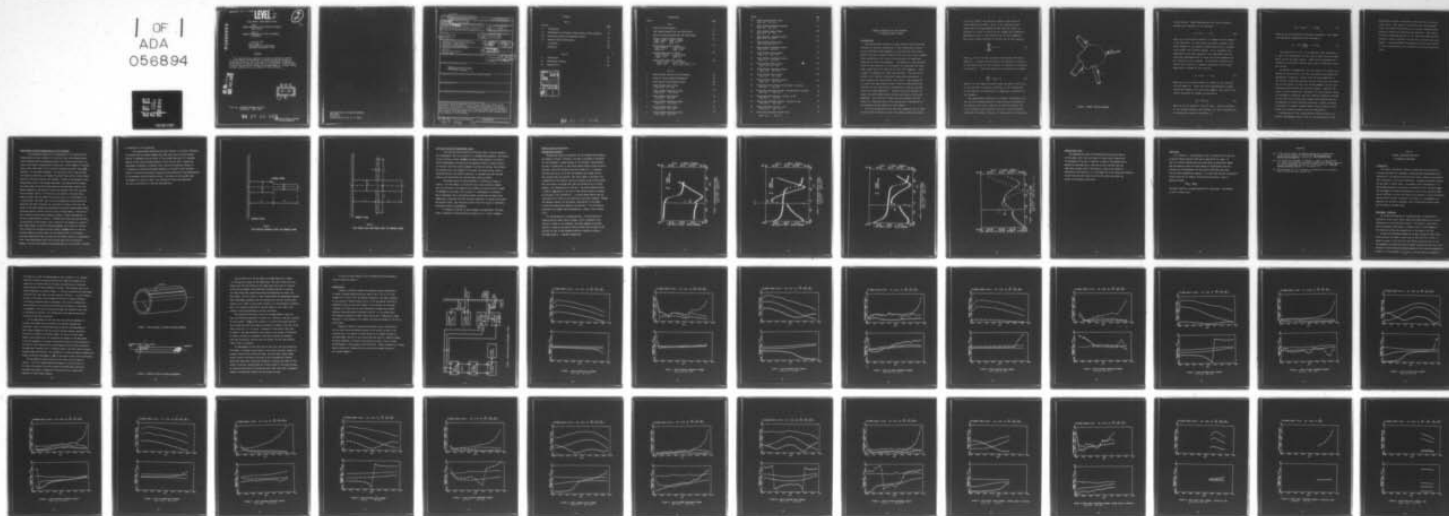
AFOSR-75-2862

UNCLASSIFIED

AFOSR-TR-78-1224

NL

1 OF 1
ADA
056894



END
DATE
FILMED

9 -78

DDC

LEVEL II**(2)**
56

FINAL REPORT AFOSR GRANT 75-2862

PART I

CHARGE CONDITION AT THE JUNCTION OF UNEQUAL
RADII WIRES

PART II

CURRENT DISTRIBUTION ON THICK CYLINDRICAL
STRUCTURES

February 1978

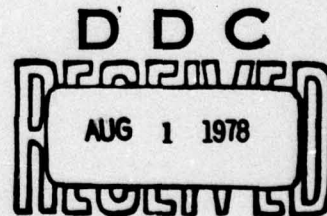
BOB M. DUFF *

THE UNIVERSITY OF MISSISSIPPI

UNIVERSITY MISSISSIPPI ,38677

ABSTRACT

This report, which is presented in two parts, presents the results of two experimental investigations of induced currents and charges on cylindrical structures. The first part is an experimental investigation of the behavior of induced charge density at the junction of unequal radii cylinders. The second part consists of the measurement of currents induced on thick cylinders and a cross composed of thick cylinders.

AD No. **DDC FILE COPY**

* Now with SOUTHWEST RESEARCH INSTITUTE
SAN ANTONIO , TEXAS 78284

78 07 26 035

Approved for public release;
distribution unlimited.

10802040A

20C LIFE COPY

Air Force Office of Scientific Research
ATTN: XOPD
Building 410
Bolling Air Force Base, D. C. 20332

UNCLASSIFIED

SECURITY CLASSIFICATION OF THIS PAGE (When Data Entered)

19 REPORT DOCUMENTATION PAGE		READ INSTRUCTIONS BEFORE COMPLETING FORM	
1. REPORT NUMBER 18 AFOSR TR- 78-1224	2. GOVT ACCESSION NO.	3. RECIPIENT'S CATALOG NUMBER	
4. TITLE (and Subtitle) CHARGE CONDITION AT THE JUNCTION OF UNEQUAL RADII WIRES. PART II. CURRENT DISTRIBUTION ON THICK CYLINDRICAL STRUCTURES.		5. TYPE OF REPORT & SERIES COVERED 9 Final rept.	
7. AUTHOR(s) 10 Bob M. Duff		8. CONTRACT OR GRANT NUMBER(s) 15 AFOSR-75-2862	
9. PERFORMING ORGANIZATION NAME AND ADDRESS Department of Electrical Engineering University of Mississippi University, Mississippi 38677		10. PROGRAM ELEMENT, PROJECT, TASK AREA & WORK UNIT NUMBERS 16 2301 A3 61102F 17 A3	
11. CONTROLLING OFFICE NAME AND ADDRESS AFOSR/NP Bolling AFB, Bldg. #410 Wash DC 20332		12. REPORT DATE 11 Feb 78	
14. MONITORING AGENCY NAME & ADDRESS (if different from Controlling Office)		13. NUMBER OF PAGES 53	
		15. SECURITY CLASS. (of this report) Unclassified 12 54 p.	
		15a. DECLASSIFICATION/DOWNGRADING SCHEDULE	
16. DISTRIBUTION STATEMENT (of this Report) Approved for public release; distribution unlimited.			
17. DISTRIBUTION STATEMENT (of the abstract entered in Block 20, if different from Report)			
18. SUPPLEMENTARY NOTES			
19. KEY WORDS (Continue on reverse side if necessary and identify by block number)			
20. ABSTRACT (Continue on reverse side if necessary and identify by block number) This report, which is presented in two parts, presents the results of two experimental investigations of induced currents and charges on cylindrical structures. The first part is an experimental investigation of the behavior of induced charge density at the junction of unequal radii cylinders. The second part consists of the measurement of currents induced on thick cylinders and a cross composed of thick cylinders.			

DD FORM 1473
1 JAN 73

EDITION OF 1 NOV 65 IS OBSOLETE

UNCLASSIFIED

SECURITY CLASSIFICATION OF THIS PAGE (When Data Entered)

409 292

Luu

Contents

Part I

Section	page
I Introduction	5
II Measurement of the surface charge density on thin cylinders	11
III Structures studied and measurement system	15
IV Measured charge distributions	16
V conclusions	22
References	23

Part II

I Introduction	24
II Measurement technique	24
III Measured data	28

ACCESSION for	
WTS	White Section <input checked="" type="checkbox"/>
BGS	Buff Section <input type="checkbox"/>
UNANNOUNCED	<input type="checkbox"/>
JUSTIFICATION	
BY	
DISTRIBUTION/AVAILABILITY CODES	
NO.	AVAIL. and/or SPECIAL
A	

28 07 26 035

Illustrations

Figure		page
Part I		
1	General Junction Geometry	7
2	Step -Radius Monopole Over the Ground Plane	13
3	Thin Cross Wire Scatterer Over the Ground Plane	14
4	Stepped - Radius Monopole Charge $a_1/\lambda = 0.00794$ $a_2/\lambda = 0.00318$ $h_1/\lambda = 0.25$ $h_2/\lambda = 0.3$	17
5	Stepped-Radius Monopole Charge $a_1/\lambda = 0.00794$ $a_2/\lambda = 0.00318$ $h_1/\lambda = 0.25$ $h_2/\lambda = 0.38$	18
6	Stepped-Radius Monopole Charge $a_1/\lambda = 0.00794$ $a_2/\lambda = 0.00318$ $h_1/\lambda = 0.25$ $h_2/\lambda = 0.5$	19
7	Unequal Radii Cross Wire Charge $a_1/\lambda = 0.00794$ $a_2/\lambda = 0.00318$ $h_1/\lambda = 0.25$ $h_2/\lambda = h_3/\lambda = h_4/\lambda = 0.5$	20
Part II		
1	Thick Cylinder Grooved for Probe Movement	26
2	Probes for Thick Cylinder Measurements	26
3	Block Diagram Of Measurement System	29
4	Thick Cylinder Axial Current $h/\lambda = 0.25$ $ka = 0.31$	30
5	Thick Cylinder Transverse Current $h/\lambda = 0.25$ $ka = 0.31$	31
6	Thick Cylinder Axial Current $h/\lambda = 0.5$ $ka = 0.31$	32
7	Thick Cylinder Transverse Current $h/\lambda = 0.5$ $ka = 0.31$	33
8	Thick Cylinder Axial Current $h/\lambda = 0.25$ $ka = 0.5$	34
9	Thick Cylinder Transverse Current $h/\lambda = 0.25$ $ka = 0.5$	35

Figure		page
10	Thick Cylinder Axial current $h/\lambda = 0.5$ $ka = 0.5$	36
11	Thick Cylinder Transverse Current $h/\lambda = 0.5$ $ka = 0.5$	37
12	Thick Cylinder Axial Current $h/\lambda = 0.75$ $ka = 0.5$	38
13	Thick Cylinder Transverse Current $h/\lambda = 0.75$ $ka = 0.5$	39
14	Thick Cylinder Axial Current $h/\lambda = 0.25$ $ka = 0.75$	40
15	Thick Cylinder Transverse Current $h/\lambda = 0.25$ $ka = 0.5$	41
16	Thick Cylinder Axial Current $h/\lambda = 0.5$ $ka = 0.75$	42
17	Thick Cylinder Transverse Current $h/\lambda = 0.5$ $ka = 0.75$	43
18	Thick Cylinder Axial Current $h/\lambda = 0.75$ $ka = 0.75$	44
19	Thick Cylinder Transverse Current $h/\lambda = 0.75$ $ka = 0.75$	45
20	Thick Cylinder Axial Current $h/\lambda = 1.0$ $ka = 0.75$	46
21	Thick Cylinder Transverse Current $h/\lambda = 1.0$ $ka = 0.75$	47
22	Thick Cross Axial Current ; Ground Plane to Junction $h/\lambda = 0.5$ $ka = 0.5$	48
23	Thick Cross Transverse Current ; Ground Plane to Junction $h/\lambda = 0.5$ $ka = 0.5$	49
24	Thick Cross Axial Current ; Junction to End $h/\lambda = 0.25$ $ka = 0.5$	50
25	Thick Cross Transverse Current ; Junction to End $h/\lambda = 0.25$ $ka = 0.5$	51
26	Thick Cross Axial Current ; Arm $h/\lambda = 0.25$ $ka = 0.5$	52
27	Thick Cross Transverse Current ; Arm $h/\lambda = 0.25$ $ka = 0.5$	53

CHARGE CONDITION AT THE JUNCTION OF UNEQUAL RADII WIRES

Introduction

The theoretical analysis of many antenna and scattering problems is greatly simplified if the conducting surfaces can be modelled using segments of electrically thin wires. These "thin wire" models usually fall into one of two classes. First portions of the actual structure may be completely replaced by thin wire segments. An example of this approach would be the analysis of an aircraft by replacing the fuselage, wings and tail sections by thin wire segments. Such a model is adequate for many applications. The second approach is to replace continuous conducting surfaces by a grid composed of electrically thin wires. The popularity of these thin wire models arises from the simplifications achieved in the theoretical formulation by making certain "thin wire approximations." Any but the very simplest of these thin wire models must contain junctions of the wire segments. The nature of these junction regions and the method of treating them in the theoretical formulation of the problem is the subject of this report.

With the assumptions that the wire segments are of electrically small radius and that the angle between the wires

is not too small, the junction region itself must be electrically very small. Thus, to be consistent with other thin wire approximations, the junction region is treated as a point at which no net charge can accumulate. Referring to Fig. 1, the currents on the wire segments must then satisfy Kirchoff's current law at the junction

$$\sum_{k=1}^N I_k = 0 \quad (1)$$

where I_k is the current entering the junction from wire number k . In many formulations of the problem a condition on the derivatives of the currents is necessary in addition to equation 1. From the equation of continuity of charge

$$\frac{dI_k}{ds} + j\omega q_s = 0 \quad (2)$$

where s is the length variable along the axis of the wire, it is seen that a junction condition on the derivatives of the currents is equivalent to imposing a condition on the charges.

The appropriate conditions on charge, consistent with the thin wire approximations, which should be imposed at the junction has been a subject of some discussion [1]. It is apparent that along the surface of any continuous conductor the surface density of charge must be continuous

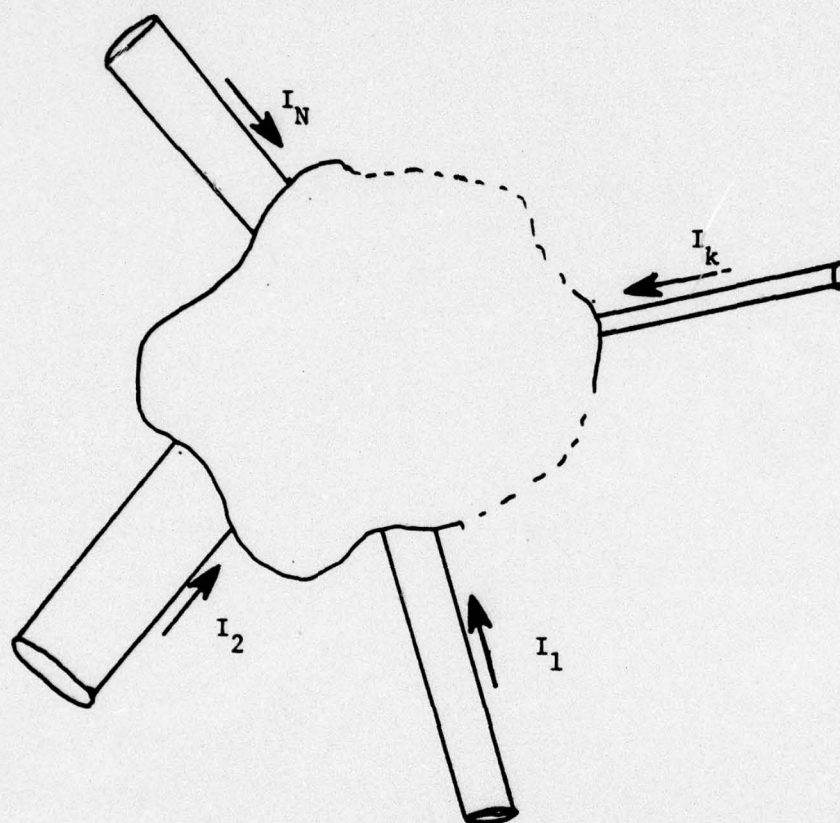


FIGURE 1 GENERAL JUNCTION GEOMETRY

at all points. Some investigators [2] have therefore imposed the condition at the junction:

$$\eta_1 = \eta_2 = \dots = \eta_n \quad (3)$$

where η_k is the surface density of charge on wire number k at the junction. On the actual structure, however, very rapid changes of the surface charge density will normally occur within the junction region. It is therefore not necessarily true that equation 3 is consistent with the thin wire approximations in which the actual geometry of the junction is not treated. An alternate junction condition [3] would be to impose continuity of the linear densities of charge at the junction

$$q_1 = q_2 = \dots = q_N \quad (4)$$

where q_k is the linear density of charge at the junction on wire number k . Since thin wire approximations assume rotational symmetry for each wire segment, the surface and linear densities of charge are related by

$$q_k = 2\pi a_k \eta_k \quad (5)$$

where a_k is the radius of the k^{th} wire. From an analysis of the tapered antenna, Wu and King [1] have proposed that an appropriate junction condition is

$$\psi_1 q_1 = \psi_2 q_2 = \dots = \psi_N q_N \quad (6)$$

where ψ_k is an appropriate expansion parameter. The expansion parameter suggested by Wu and King is

$$\psi_k = 2 \left[\ln \left(\frac{2}{ka_k} \right) - 0.5772 \right] \quad (7)$$

From equations 5 and 7 it is apparent that equations 3, 4, and 6 are equivalent for the case in which all wire segments are of the same radius. These three junction conditions are different however when wires of different radii are joined.

It should be emphasized that the need for a charge condition at the junction, and the controversy concerning the appropriate condition, arises from the approximation of the actual conducting surfaces by thin wires and the inability of this model to treat the actual geometry of the conducting surface within the junction region. Another feature, of most theoretical treatments of this problem, which is intimately connected with the junction condition problem is the fact that current and charge distributions must be represented by slowly varying functions. Hence the rapid variations of surface charge density which actually occur within the junction region are not represented.

The purpose of the investigation reported here is to obtain experimental data to aid in the definition of the

appropriate charge conditions at the junction of unequal radii wires. Two types of structure were investigated. First the charge distribution on a driven stepped-radius monopole antenna was measured and analyzed. The second structure investigated was a wire cross scatterer having different radii cylinders for the main stem and the cross member. The measurement techniques used and the results of this investigation are presented in the following sections.

Measurement of Surface Charge Density on Thin Cylinders

The conventional method for the measurement of the induced surface charge density on thin cylinders is to utilize a very short monopole probe which protrudes from the conducting surface. The voltage induced across the load of this probe is proportional to the electric field tangent to the probe, hence to the field normal to the surface of the test structure. The boundary condition, on the normal component of the electric field, then provides the necessary proportionality between the probe signal and the surface charge density on the test structure. Two problems, related to the response of the charge probe, arise in the present experiment. The proportionality between the probe signal and surface charge requires that the probe respond to the normal component of the electric field at the surface of the test structure. Since the probe itself is of finite size, the electric field must either remain constant over the length of the probe or vary in a known manner. On a long cylinder the field near the surface is radially directed and varies inversely with radial distance. This variation of electric field over the length of the probe changes the proportionality constant between probe signal and charge density. Correct relative values of charge density from point to point along the surface may be measured, however, without determination of the exact proportionality constant. A problem arises when the probe approaches a discontinuity in the surface, such as the end of the antenna or a junction. Near these changes in the test structure geometry the variation of electric field strength with distance from the surface changes and hence so does the relation between the probe signal and the charge density. In the present experiment measurements near the junction are therefore subject to considerable error. Exact measurements within the junction region are not necessary, however, since only the smoothly extrapolated behavior of the charge is desired

as explained in the introduction.

The second problem concerning the probe response is of greater importance. The proportionality constant between the probe signal and the surface charge density is dependent upon the radius of the cylinder upon which it is mounted because of the inverse distance behavior of the electric field. Before the measurements conducted on different radii wires can be correctly related, it is necessary to calibrate the probe response as a function of test structure radius. An extensive experimental program has been conducted for the determination of the necessary probe calibration factors. The results of this project were the subject of a previous report. The calibration factors thus determined are used in the analysis of the data presented here.

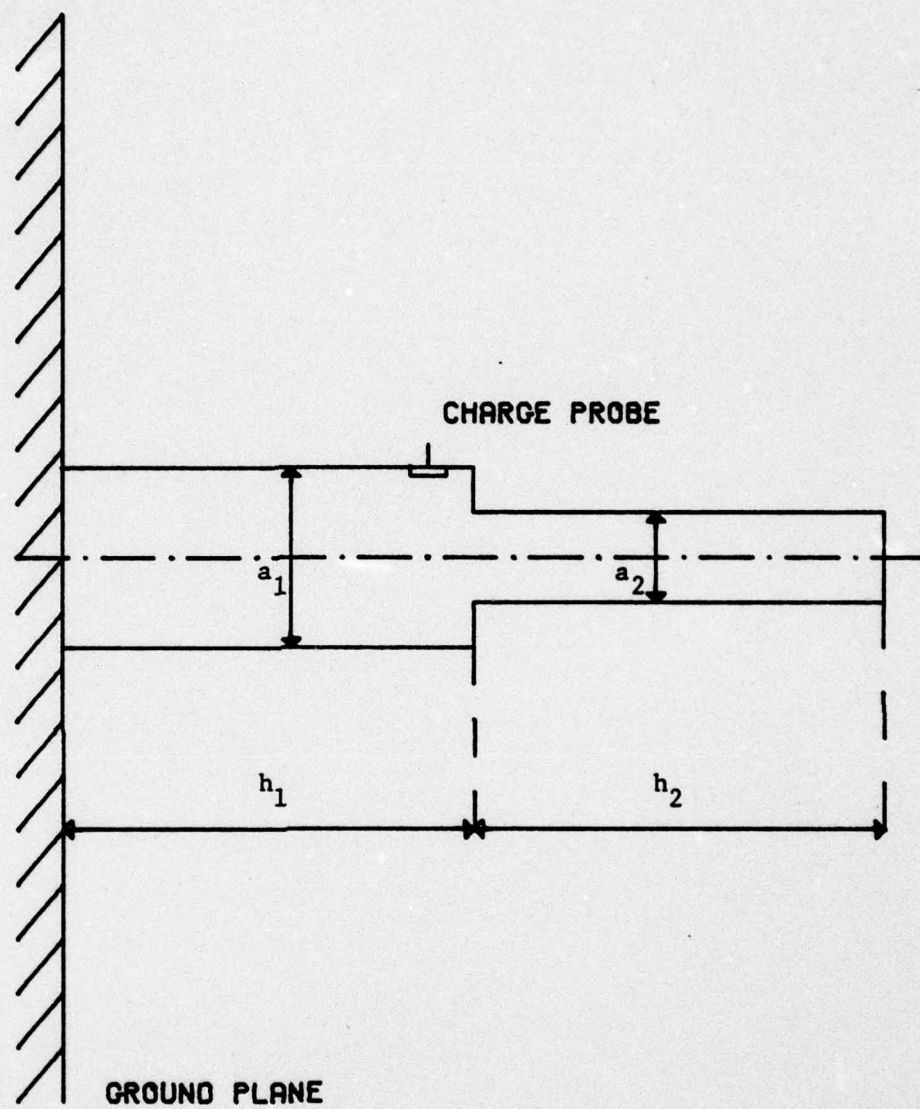


FIGURE 2
STEP RADIUS MONOPOLE OVER THE GROUND PLANE

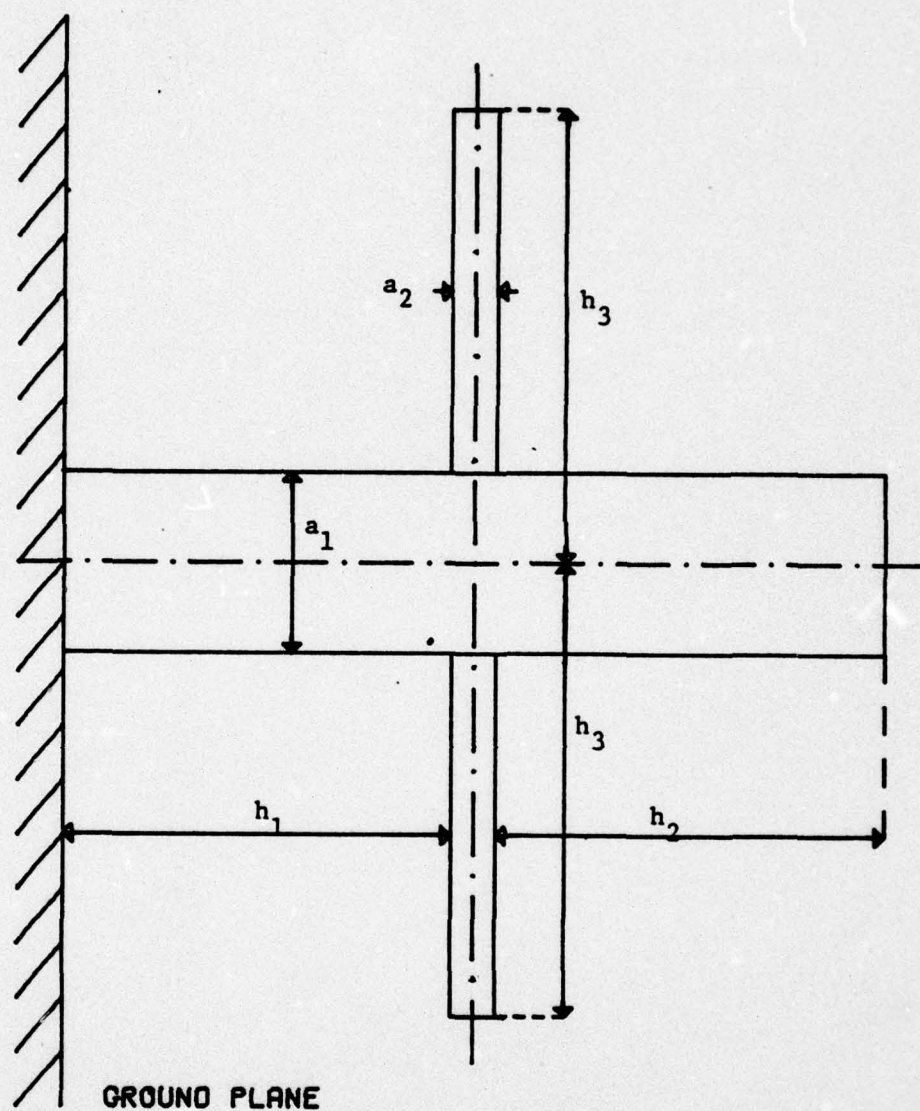


FIGURE 3
THIN CROSS WIRE SCATTERER OVER THE GROUND PLANE

Structures Studied and Measurement System

Test structures which contain two different types of junction geometry are investigated. The first structure is a stepped-radius monopole. The junction of this structure is thus simply two cylinders joined coaxially, as shown in figure 2. Measurements are made with the monopole driven by a coaxial anulus at its base. Since only axially symmetric currents are excited, the cylinders are slotted axially for movement of the probe. The probe carriage, which is contained inside of the tubular conductors, is designed such that the same probe can be used on both the large and small radius cylinders.

The second type of structure examined is a 90° cross, as shown in figure 3. The cross member is of smaller radius than the vertical member, and as in the case of the monopole the cylinders are slotted axially to allow for movement of the probe. This structure is investigated as a scatterer, being illuminated from a transmitting antenna located near the edge of the image plane. Since both axial and tranverse components of current exist within the junction region, the conducting surface within this region is maintained continuous during the measurements.

A frequency of 300 MHz is used throughout the experiment. The probe signal is measured in both amplitude and phase by a R.F. vector voltmeter.

Measured Charge Distributions

Stepped-Radius Monopole

The measured charge distributions for the stepped-radius monopole are shown in figures 4 through 6. The data as presented is corrected for the difference in probe response on the different radii cylinders and thus is proportional to the surface charge density along the entire structure. The axial distance along the cylinders, "s", is measured from the junction. As can be seen the measured data changes rapidly with distance near the junction. This rapid change is believed to be a combination of two factors, the true variation of the surface charge near the junction and probe error near the discontinuity in surface geometry. For interpretation of the data, the values measured within a region of approximately five radii of the junction should be ignored. As discussed in the introduction, the surface charge density must be continuous at all points on an electrically continuous conductor. However, the important feature for the present investigation is the manner in which the charge would behave at the junction if the distribution along each wire segment were represented by a smooth, slowly varying curve.

For interpretation of the measured data, the distribution of charge along the larger radius cylinder, ($s < 0$), projected to the junction is taken as the reference. The points at which the surface density of charge on the smaller radius cylinder would project to the junction for each of the proposed conditions, equations 3, 4 and 6, have been shown as q and ψq respectively.

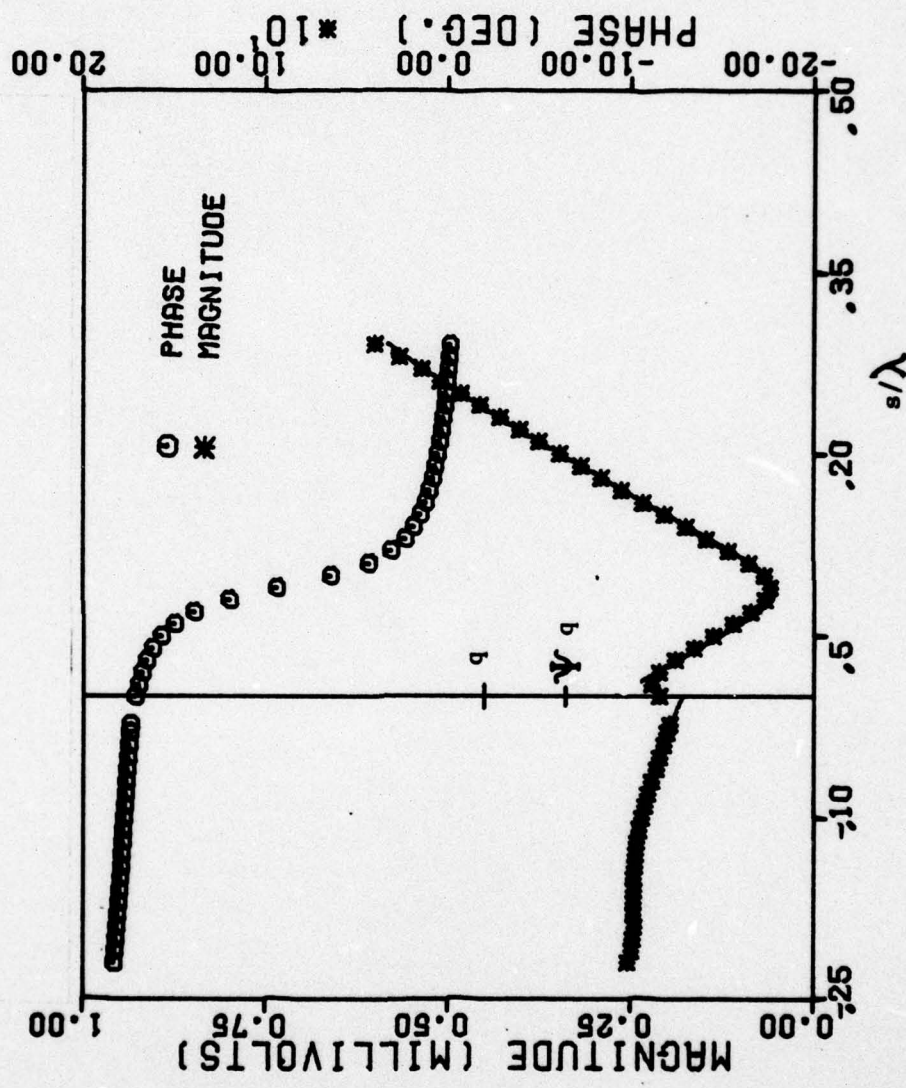


FIGURE 4 STEPPED-RADIUS MONOPOLE CHARGE
 $a_1/\lambda = 0.00794$ $a_2/\lambda = 0.00318$
 $h_1/\lambda = 0.25$ $h_2/\lambda = 0.3$

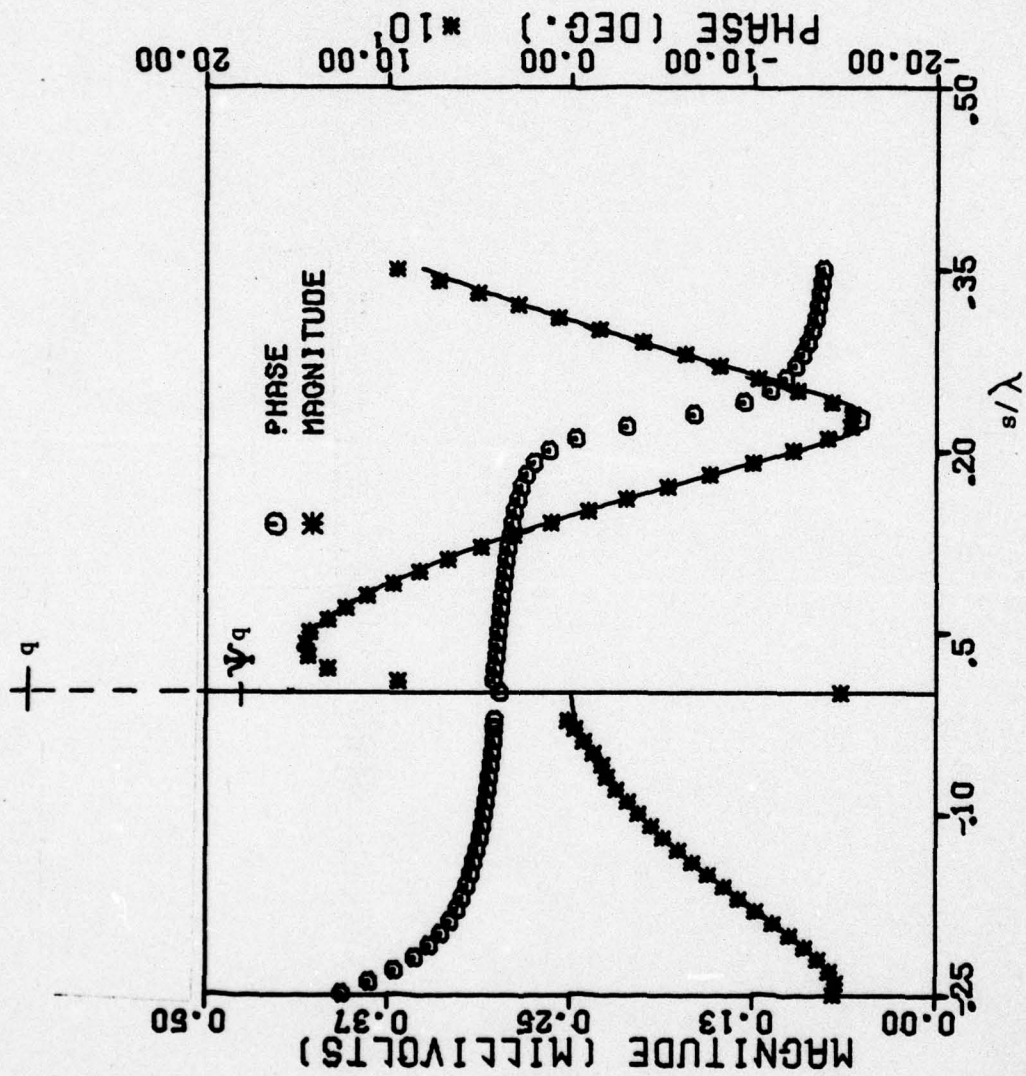


FIGURE 5 STEPPED-RADIUS MONOPOLE CHARGE
 $a_1/\lambda = 0.00794$ $a_2/\lambda = 0.00318$
 $h_1/\lambda = 0.25$ $h_2/\lambda = 0.38$

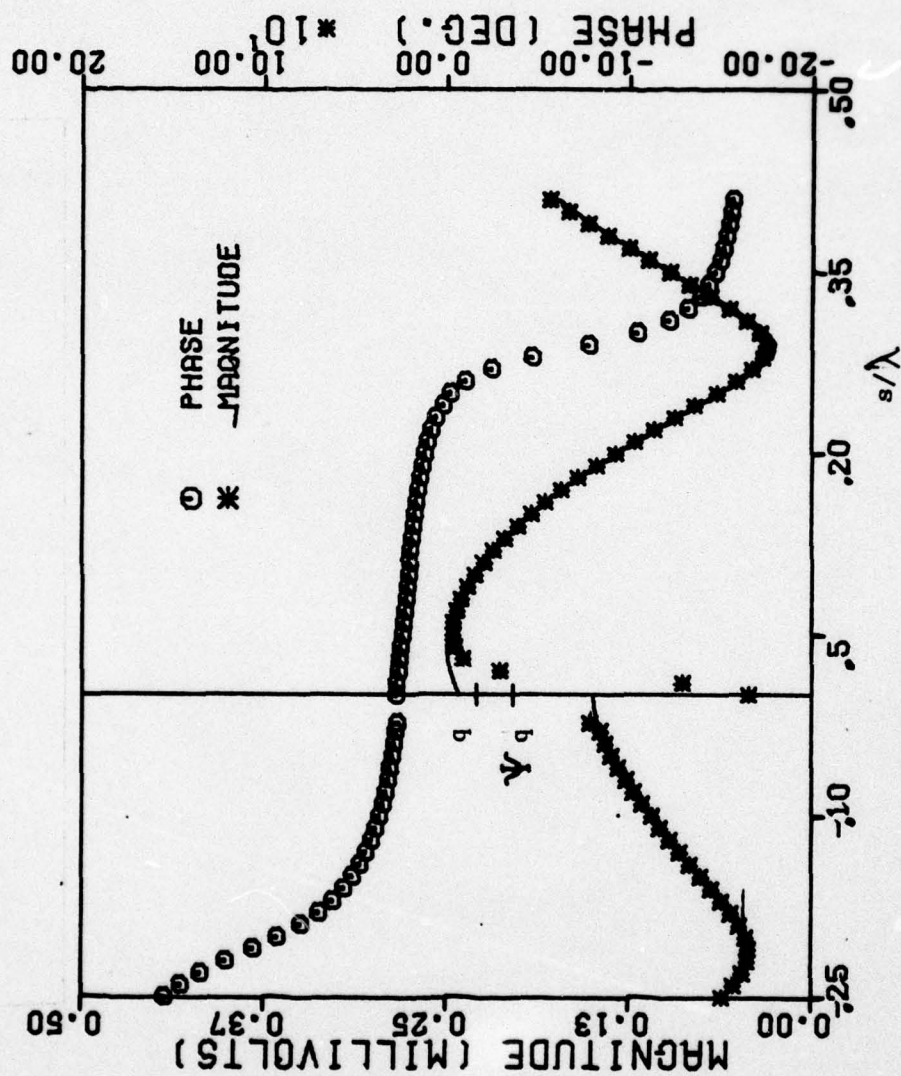


FIGURE 6 STEPPED-RADIUS MONOPOLE CHARGE
 $a_1/\lambda = 0.00794$ $a_2/\lambda = 0.00318$
 $h_1/\lambda = 0.25$ $h_2/\lambda = 0.5$

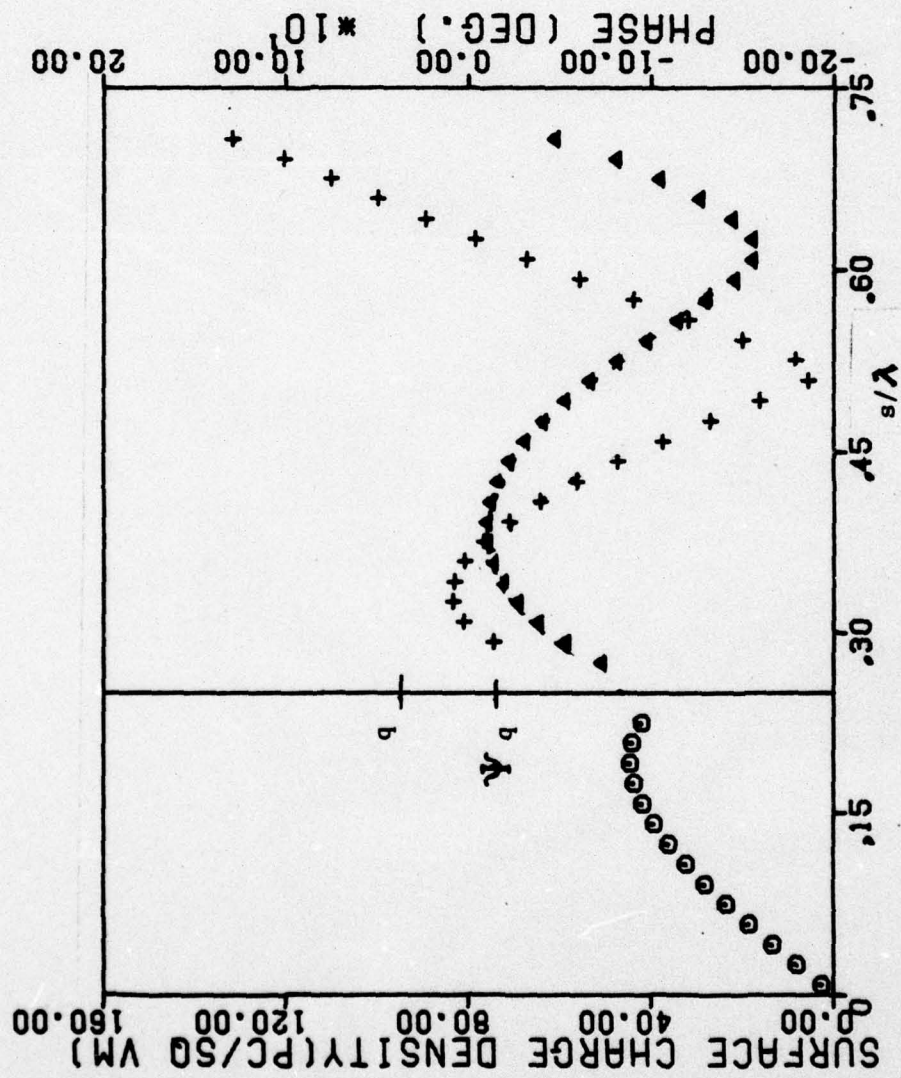


FIGURE 7 UNEQUAL RADII CROSS WIRE CHARGE
 $a_1/\lambda = 0.00794$ $a_2/\lambda = 0.00318$
 $h_1/\lambda = 0.25$ $h_2/\lambda = h_3/\lambda = h_4/\lambda = 0.5$

Unequal Radii Cross

The magnitude and phase of the measured surface charge density on the unequal radii cross are shown in figures 7 and 8 respectively. The treatment of the data is identical to that of the stepped-radius monopole as described above. Since the vertical sections have the same radius on both sides of the junction, these curves should be continuous at the junction. It is the comparison of the charge distributions on the cross arms with those on the vertical arms which shows the effects of the junction conditions.

Conclusions

It is difficult , from expeimental data, to establish with certainty a junction charge condition which may be applied for all cases. In fact it is obvious thatthe consition which should be applied may depend upon the degree to which the rapid change of charge density near the junction can be represented with the solution technique being used. From the data presented here however, it is clear that the most consistently correct condition for smoothly extrolated distributions is that of equation 6,namely

$$\psi_1 q_1 = \psi_2 q_2$$

The other conditions ,although appropriate for some cases , are greatly in error in other cases.

References

- [1] T.T.Wu and R.W.P.King, "The Tapered Antenna and its Application to the Junction Problem for Thin Wires", IEEE Transactions on Antennas and Propagation, Vol.AP-24, pp. 42-45, January 1976.
- [2] E. K. Miller, R.M. Bevensee, A.J. Poggio, L. Adams, F.J. Deadrick and J.A. Landt, "An Evaluation of Computer Programs Using Integral Equations for the Electromagnetic Analysis of Thin Wire Structures", AFWL EMP Interaction Notes, Note 177, p. 104, March 1974
- [3] R.W.P.King and T.T. Wu, "Analysis of Crossed Wires in a plane Wave Field." Interaction Note 216, July 1974

PART II

CURRENT DISTRIBUTION ON THICK CYLINDRICAL STRUCTURES

Introduction

The current distribution induced on electrically thin cylindrical structures has been very thoroughly investigated both experimentally and theoretically. The problem of defining the currents induced on electrically thick structures is not so well understood, although considerable progress has been made in recent years. The purpose of the investigation is to provide measured data on cylindrical structures of radii for which $ka \leq 1$. The investigation includes measurements on single, finite length cylinders and on a 90° cross. The cross was chosen as an example of a thick cylindrical structure which contains a junction of cylinders. All measurements are made with the structure illuminated from a transmitting antenna located near the edge of the image plane.

Measurement Technique

The current distribution on a conducting body is conventionally measured by using a small center loaded loop probe mounted with its plain perpendicular to the conducting surface. If the probe is sufficiently small and properly constructed it responds to the H field tangent to the conducting surface and perpendicular to the plane of the loop.

An important difference between the currents induced on electrically thick cylinders from those on thin wires is that the thick cylinder can support currents in both the axial and transverse directions. Each of the two components of current can have an angular variation as well as an axial variation in both amplitude and phase. Because of the transverse component of current it is not possible to cut a slot in the cylinder for movement of

the probe as is usual for measurements on thin cylinders. It is therefore necessary to design a probe system which will allow for movement of the probe over the surface while at the same time maintaining a continuous conducting path for both components of current. The technique used in the present experiment is shown in figure 1. The test structures are constructed from thick wall brass tube. An axial groove is milled in , but not through , the wall of the tube. Thus although the surface is slightly disturbed , a continuous conducting path is maintained. Later tests confirmed that the disturbance of the current distribution by the groove in the surface is negligible. Thin strips of brass shim stock are soldered to each side of the groove to provide a slot through which the probe may move while being held flush with the surface.

For the measurement of both the axial and transverse components of current, loop probes must be oriented in two mutually perpendicular directions. Ideally a single probe would be used for the measurement of both current components, since this would eliminate problems concerning the relative response of different probes. The use of a single probe however, would require that its orientation be changed for the measurement of the two components of current. The accuracy required in the orientation of the probe is very high, particularly when measuring the transverse component. The mechanical construction of a rotatable probe in the small space available presents severe difficulties. The alternative of using two mutually perpendicular probes has definite advantages in spite of the need for their mutual calibration.

The two probes are constructed on a thin brass strip, as shown in figure 2. This strip extends behind the probes to a position which in all cases is outside of the test structure. The probes were constructed from semi-rigid coaxial transmission line having a solid copper outer conductor of 0.023 inches diameter.

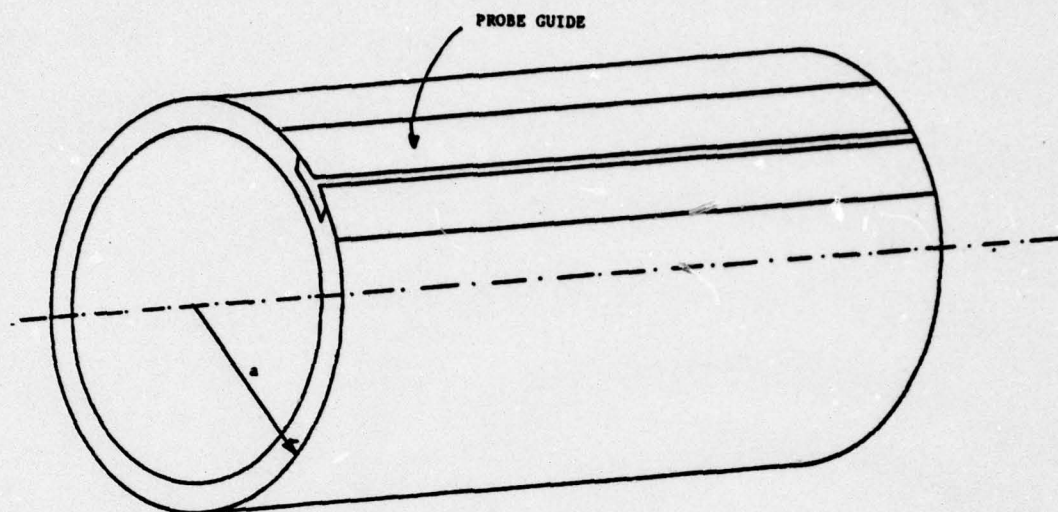


FIGURE 1 THICK CYLINDER - GROOVED FOR PROBE MOVEMENT

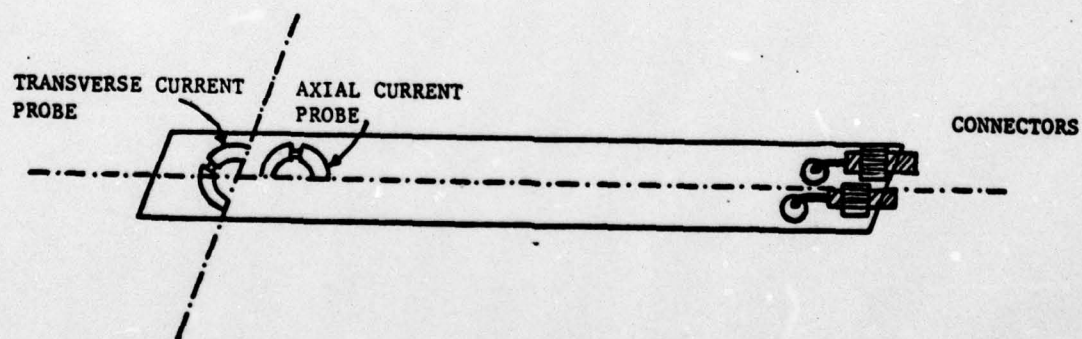


FIGURE 2 PROBES FOR THICK CYLINDER MEASUREMENTS

The calibration of the two probes is accomplished with a special test fixture which mounts on the image plane. This test fixture holds the probes flush with the surface of the image plane but allows for rotation of the entire assembly. The calibration procedure consists of orienting one probe toward the transmitting antenna and measuring the signal from both probes. The test fixture is then rotated 90° and the measurement repeated. These measurements, together with the orientations of the test fixture which produce a null signal on each probe, provide all of the necessary calibration data. This relative calibration of the two probes is later used in the analysis of the data measured on the test structures.

The system described above allows for the measurement of both the axial and transverse components of current as a function of the axial position on the cylinders. To obtain the variation of current with angular position the cylinder upon which the probes are mounted is rotated. In the case of the cross structure it is, of course, necessary for the plane of the cross to remain in the same orientation with respect to the incident illumination. In order to achieve this orientation the junction section was designed such that the vertical sections could be rotated but the cross sections remain fixed in orientation.

For measurements on the outer arms of the cross, the strip containing the probes is arranged to bend inward at the junction and pass through the junction inside of the cylindrical tubes. Thus the signal cables always passed inside of the tubular structure to the instrumentation located behind the image plane. Tests were conducted to determine the effect of the groove in the test structure and the sliding contact of the probe carriage by covering these areas with conducting tape. These tests show a negligible change in the measured current with and without the tape.

An over all block diagram of the instrumentation and measurement system is shown in figure 3.

Measured Data

Figures 4 through 21 present the measured current distributions on single cylinders having electrical radii of $ka = 0.31$ to 0.75 , and lengths of $h = 0.25$ to 1.0 . The angular variation of the axial component of the current is clearly evident. For $h = 0.25$ the angular variation is essentially $\cos \phi$ over the entire length of the cylinder. As the length increases it is seen that the axial distribution changes with angular position, being particularly different at $\phi = 0$ (i.e. the shadow side). The transverse component is small except near $\phi = 90$, (indicating a $\sin \phi$ variation). This component also exhibits the expected maximum at the end of the cylinder.

Figures 22 through 27 present the measured current distributions for the cross structure. Currents induced on the vertical portion of the cross are seen to be similar to those induced on a straight cylinder of the same length. Effects of the junction and side arms are , however, evident. The axial component of current in the side arm is seen to have a strong $\sin \phi$ component , being largest at $\phi = 90$ and 270 . These currents are of course induced entirely by coupling from the currents and charges induced on the vertical members.

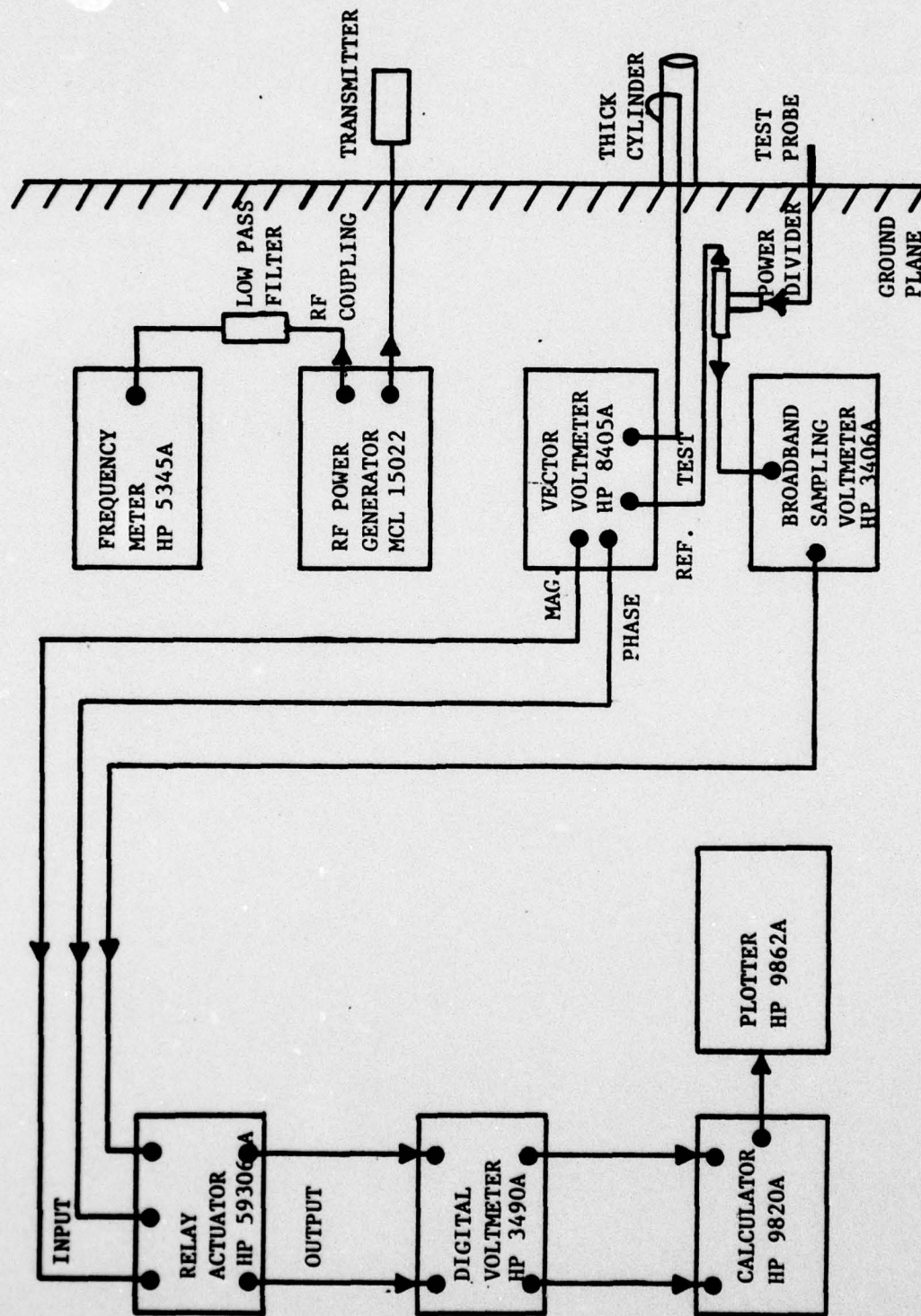


FIGURE 3 BLOCK DIAGRAM OF MEASUREMENT SYSTEM

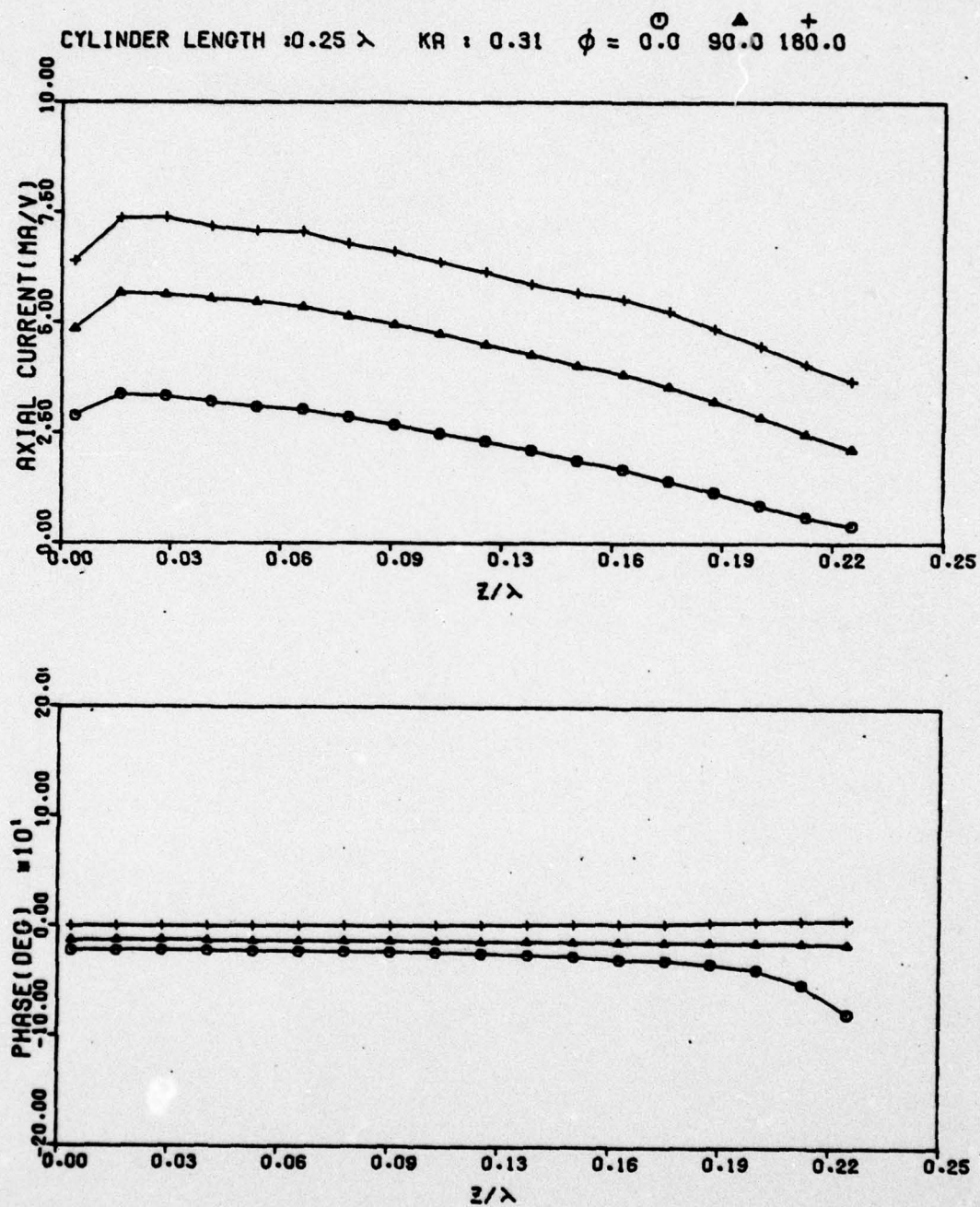


FIGURE 4 THICK CYLINDER AXIAL CURRENT
 $h/\lambda = 0.25$ $ka = 0.31$

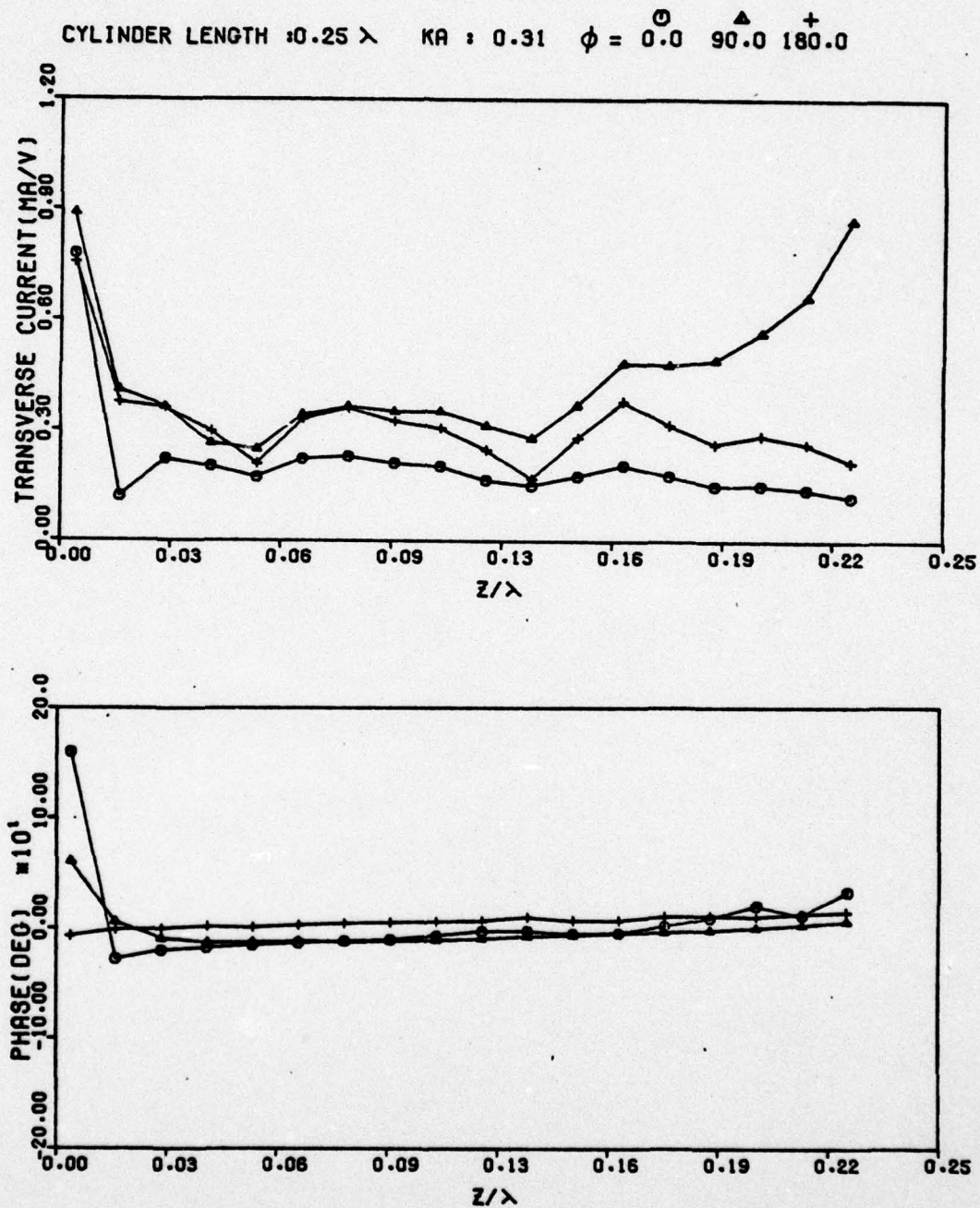


FIGURE 5 THICK CYLINDER TRANSVERSE CURRENT
 $h/\lambda = 0.25$ $ka = 0.31$

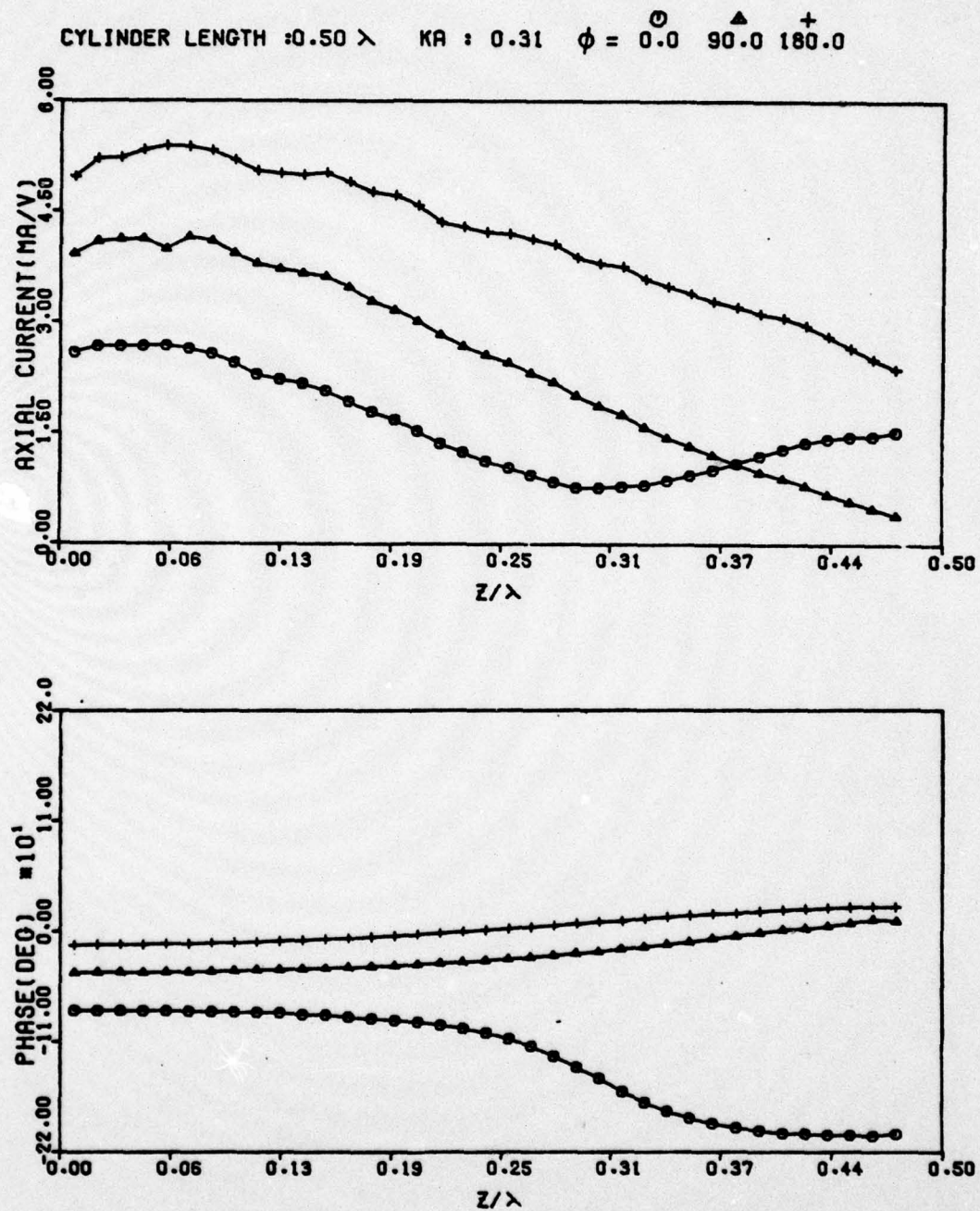


FIGURE 6 THICK CYLINDER AXIAL CURRENT
 $h/\lambda = 0.5$ $ka = 0.31$

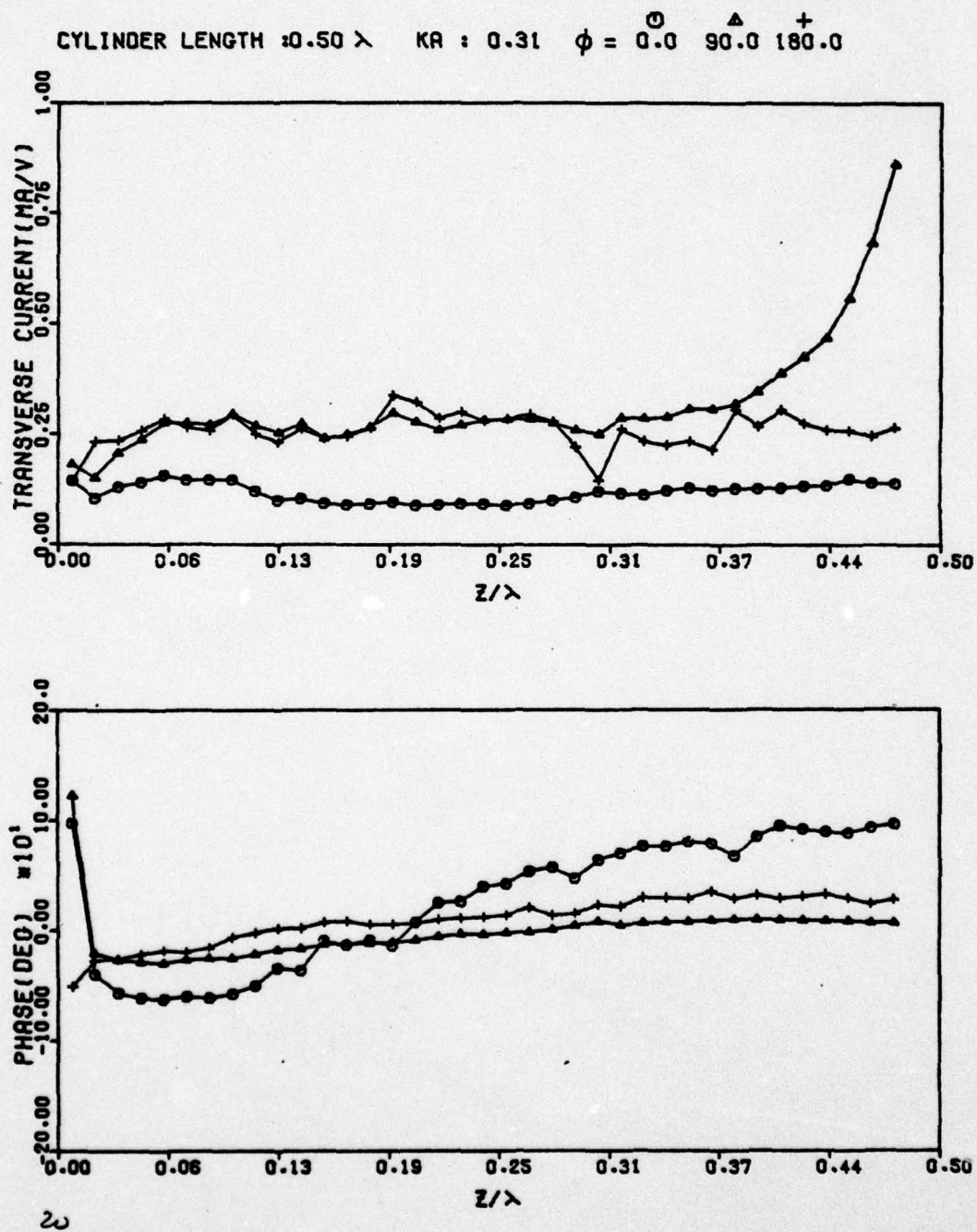


FIGURE 7 THICK CYLINDER TRANSVERSE CURRENT
 $h/\lambda = 0.5$ $ka = 0.31$

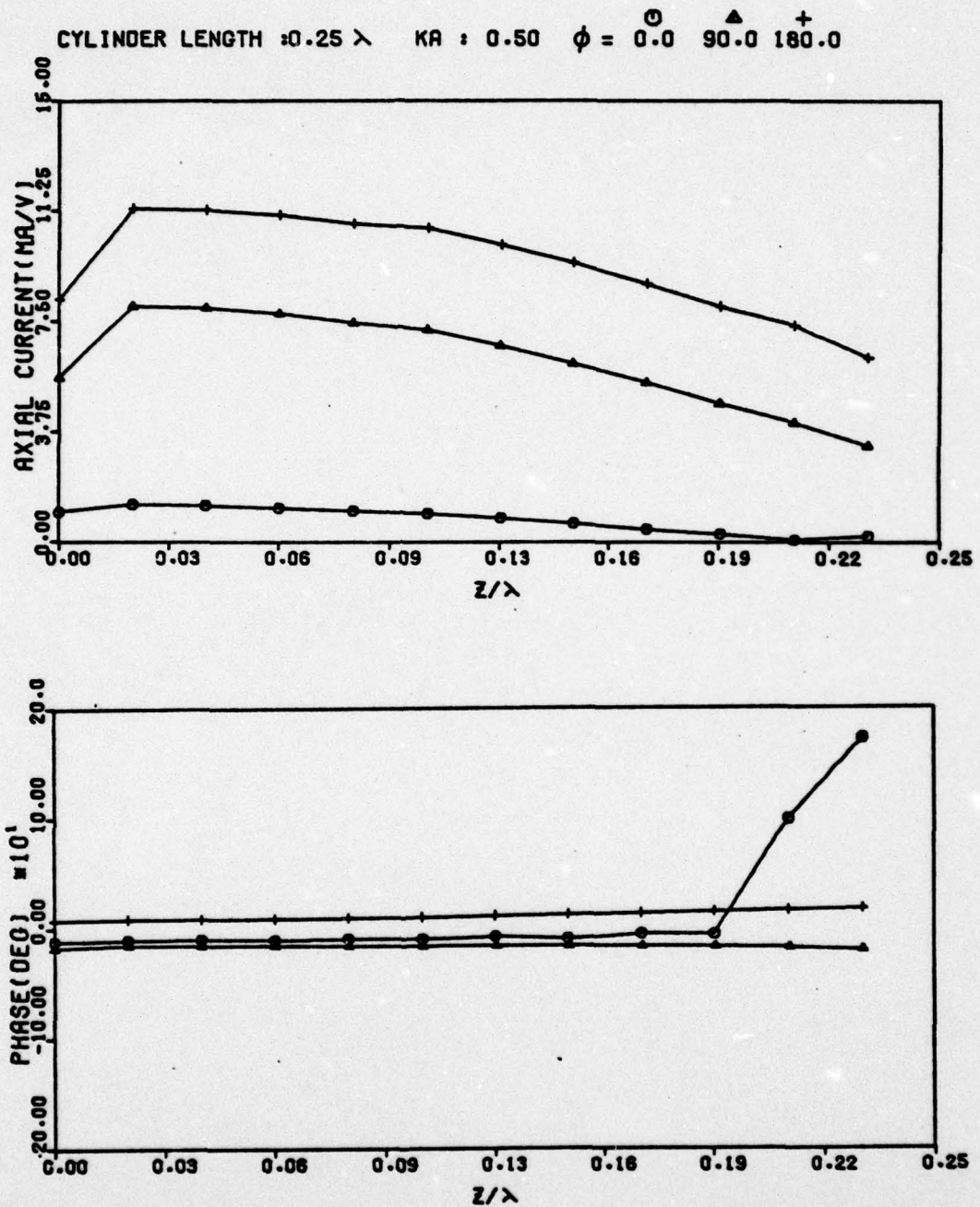


FIGURE 8 THICK CYLINDER AXIAL CURRENT
 $h/\lambda = 0.25$ $ka = 0.5$

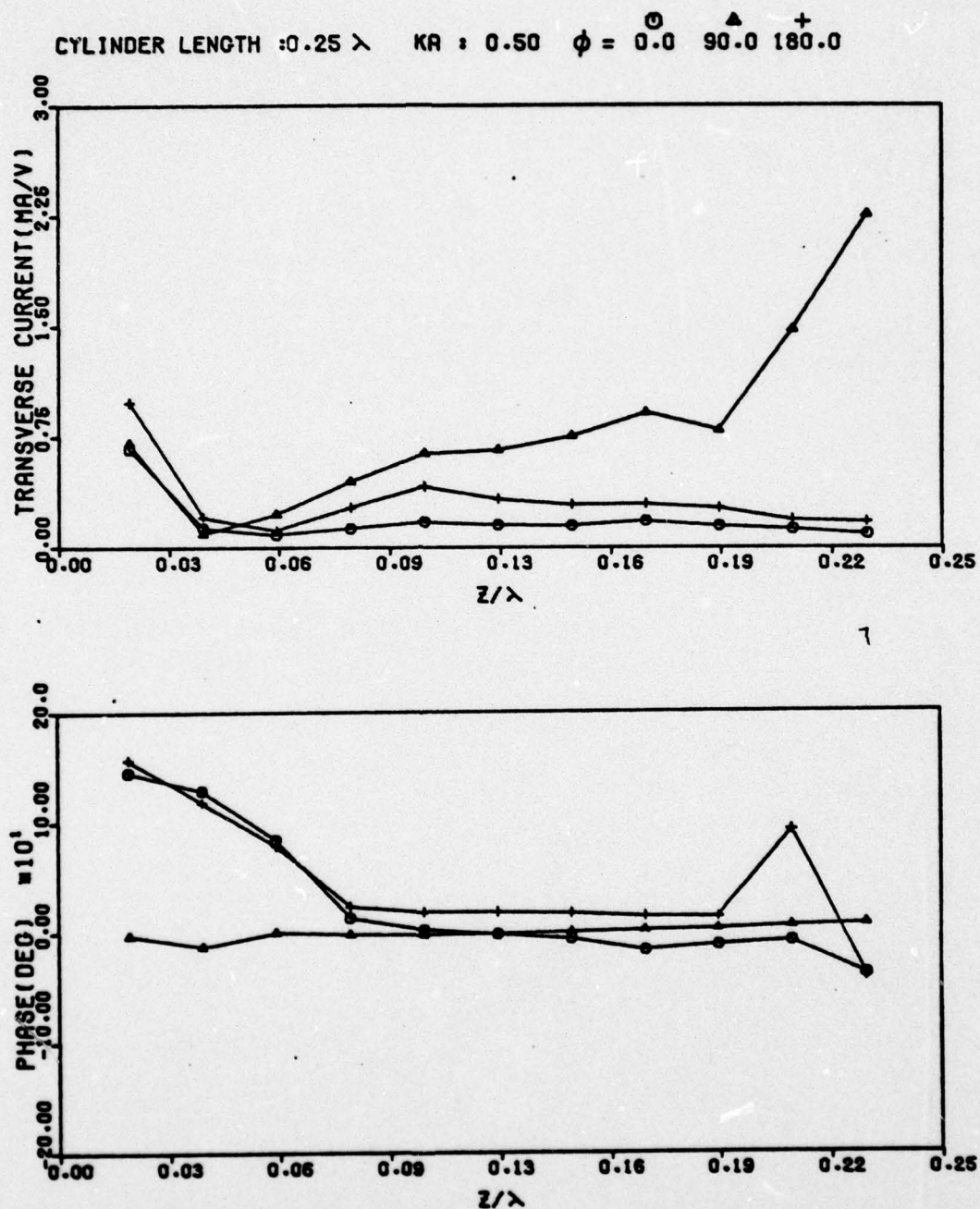


FIGURE 9 THICK CYLINDER TRANSVERSE CURRENT
 $h/\lambda = 0.25$ $ka = 0.5$

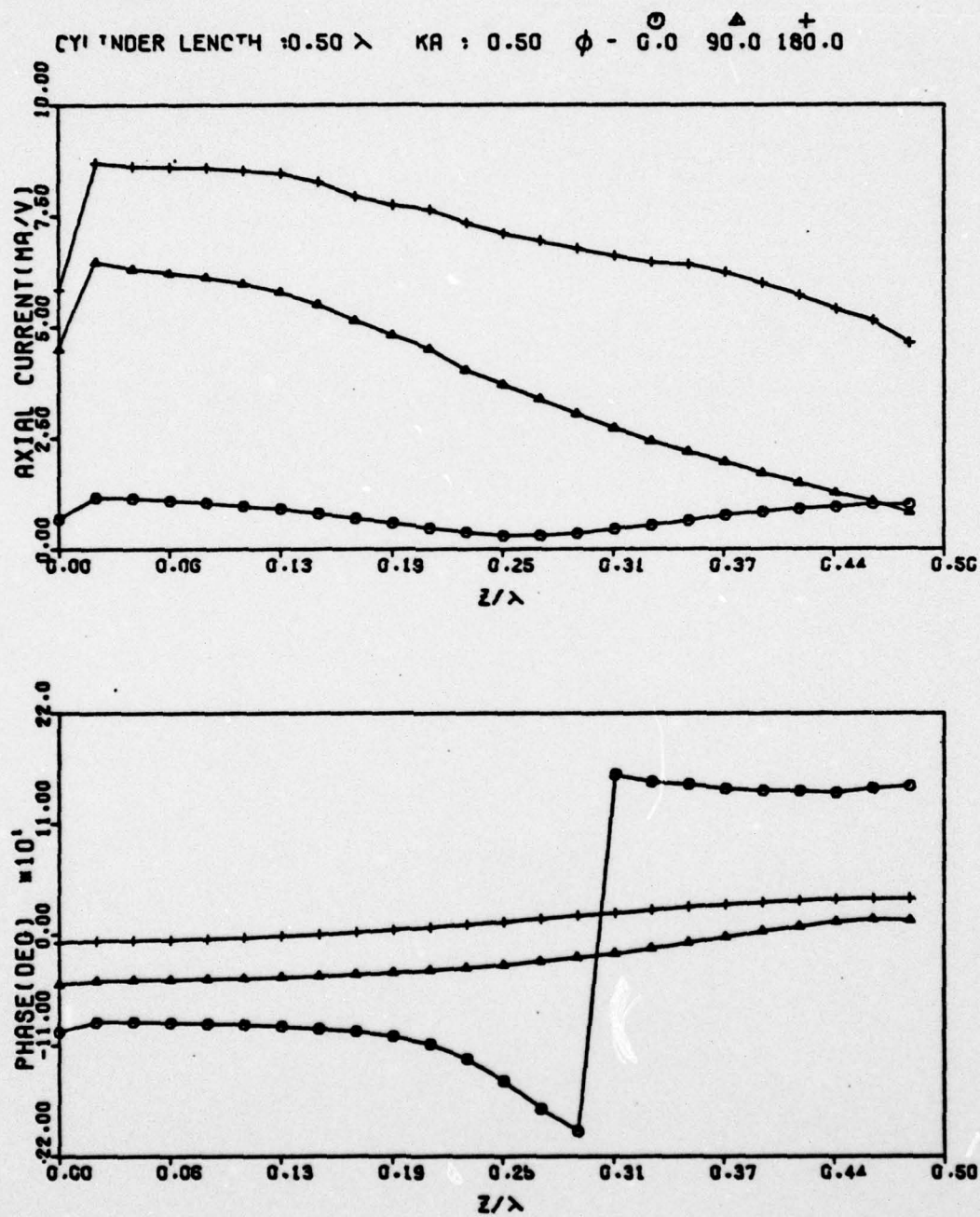


FIGURE 10 THICK CYLINDER AXIAL CURRENT
 $h/\lambda = 0.5$ $ka = 0.5$

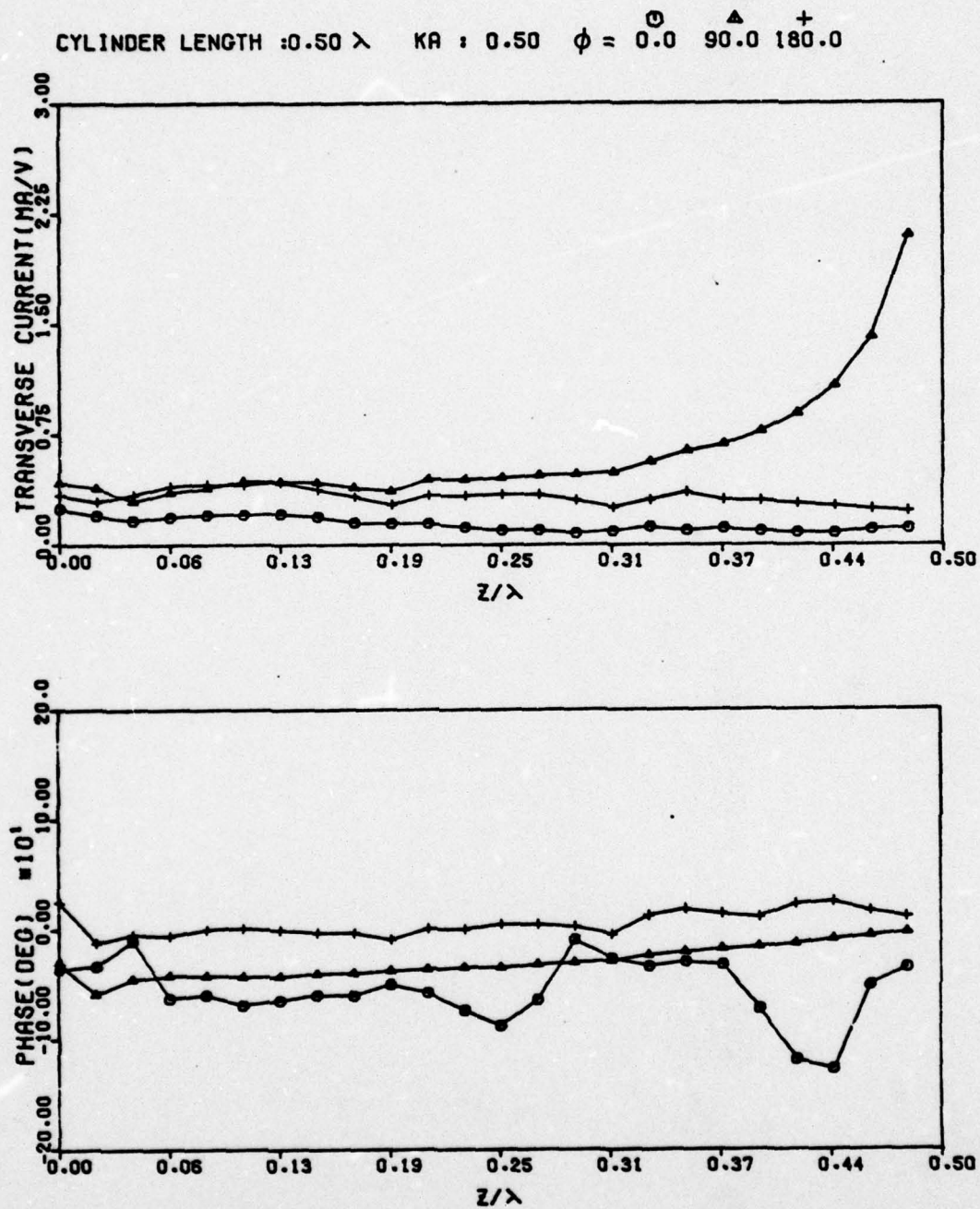


FIGURE 11 THICK CYLINDER TRANSVERSE CURRENT
 $h/\lambda = 0.5$ $ka = 0.5$

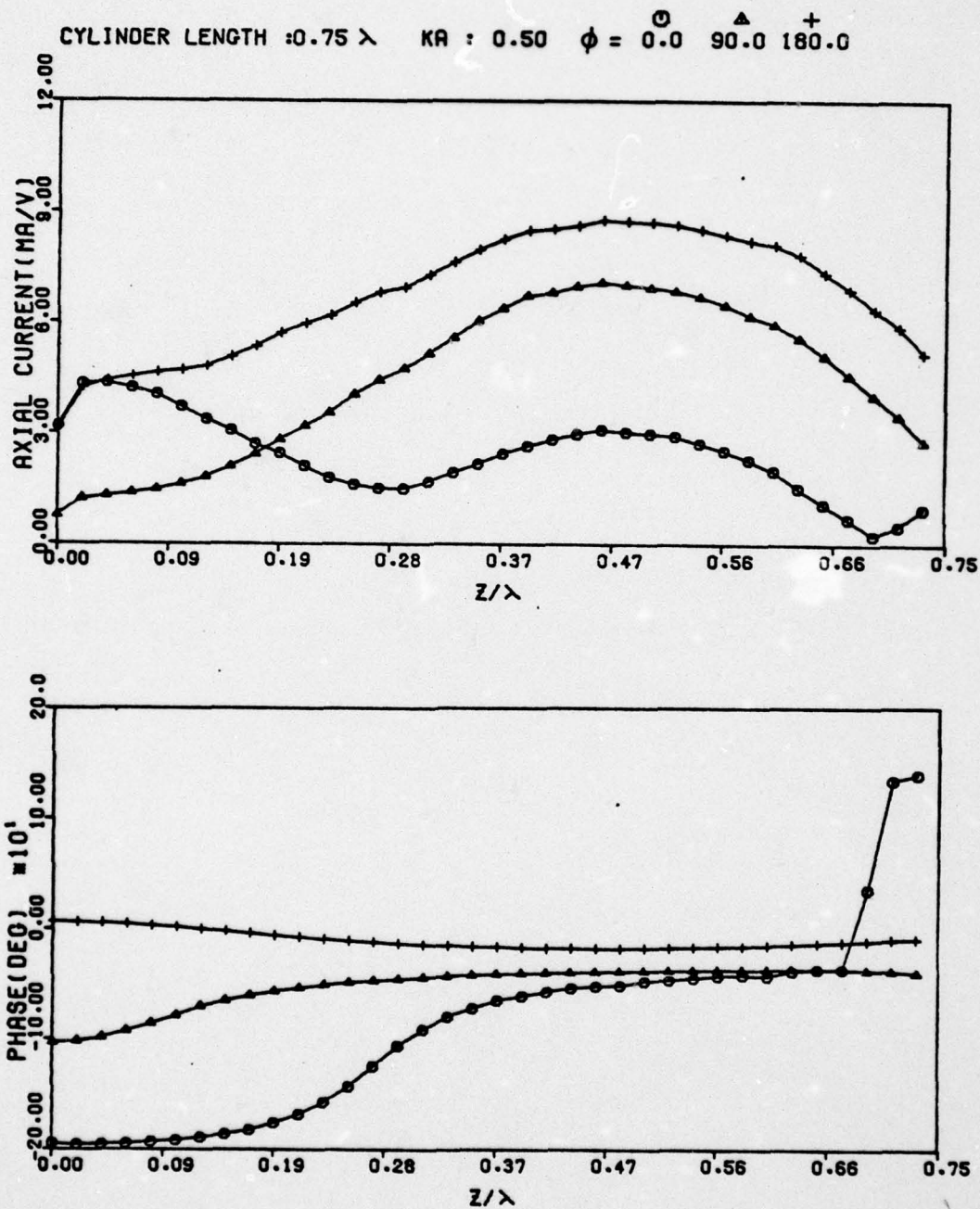


FIGURE 12 THICK CYLINDER AXIAL CURRENT
 $h/\lambda = 0.75$ $ka = 0.5$

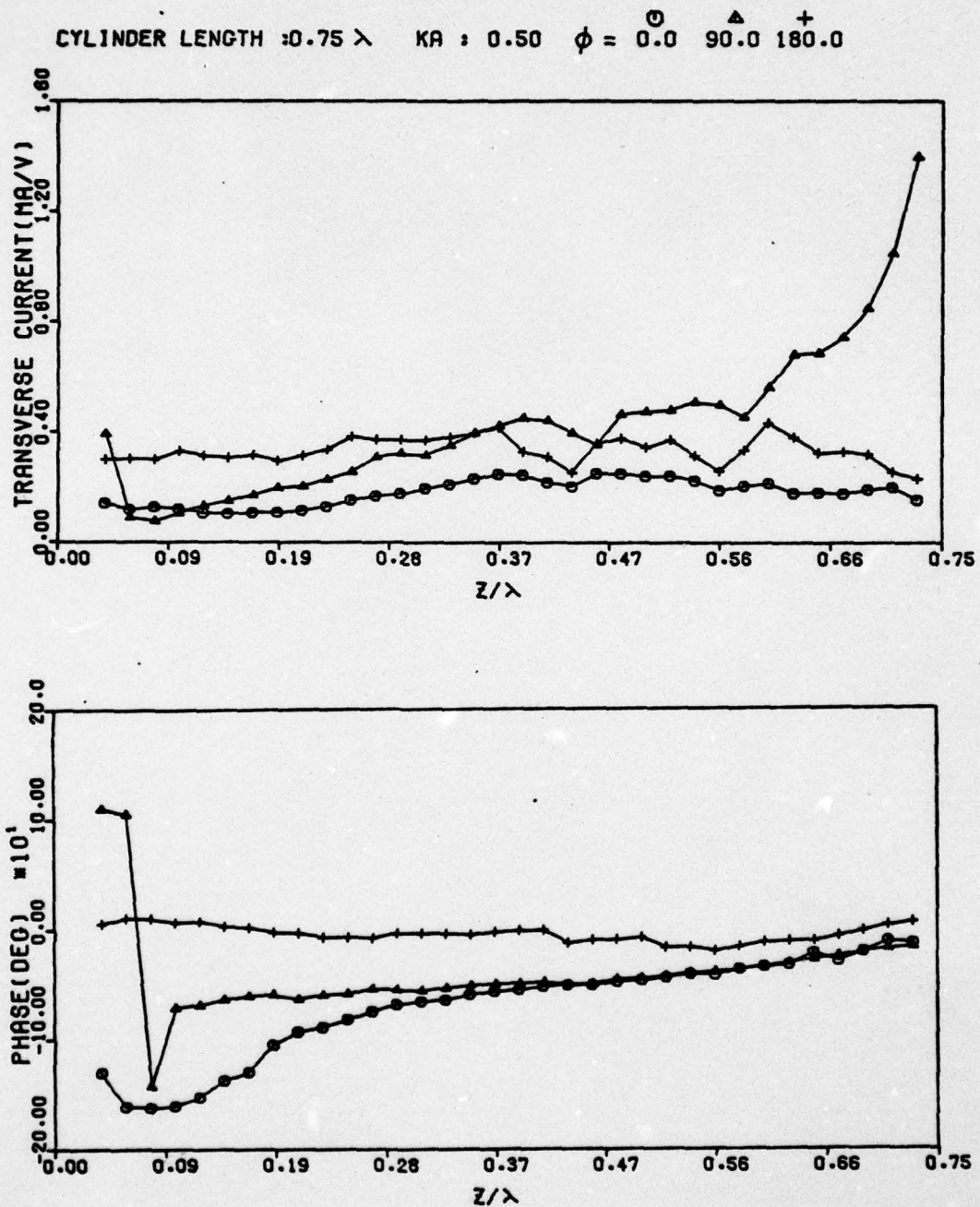


FIGURE 13 THICK CYLINDER TRANSVERSE CURRENT
 $h/\lambda = 0.75$ $ka = 0.5$

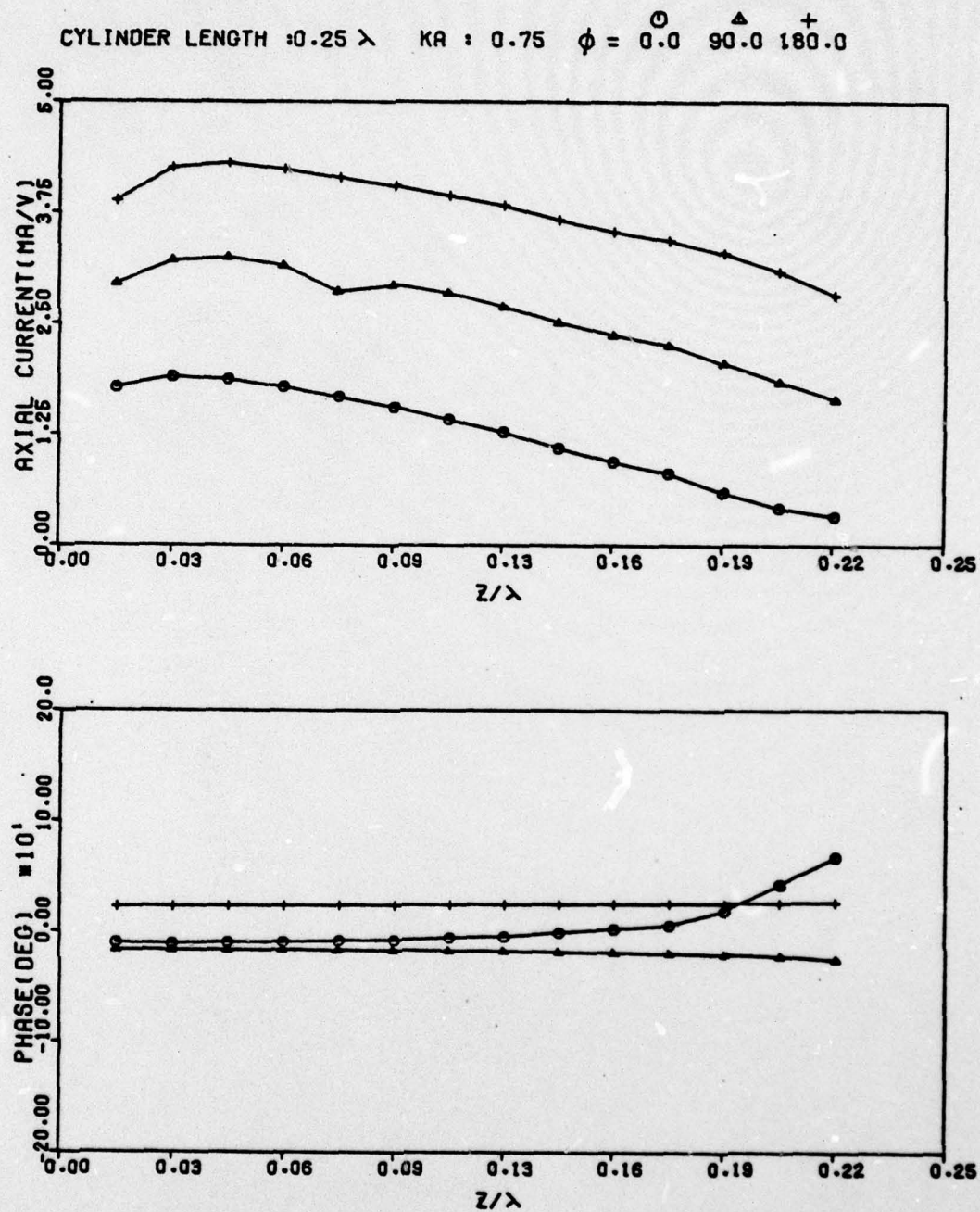


FIGURE 14 THICK CYLINDER AXIAL CURRENT
 $h/\lambda = 0.25$ $ka = 0.75$

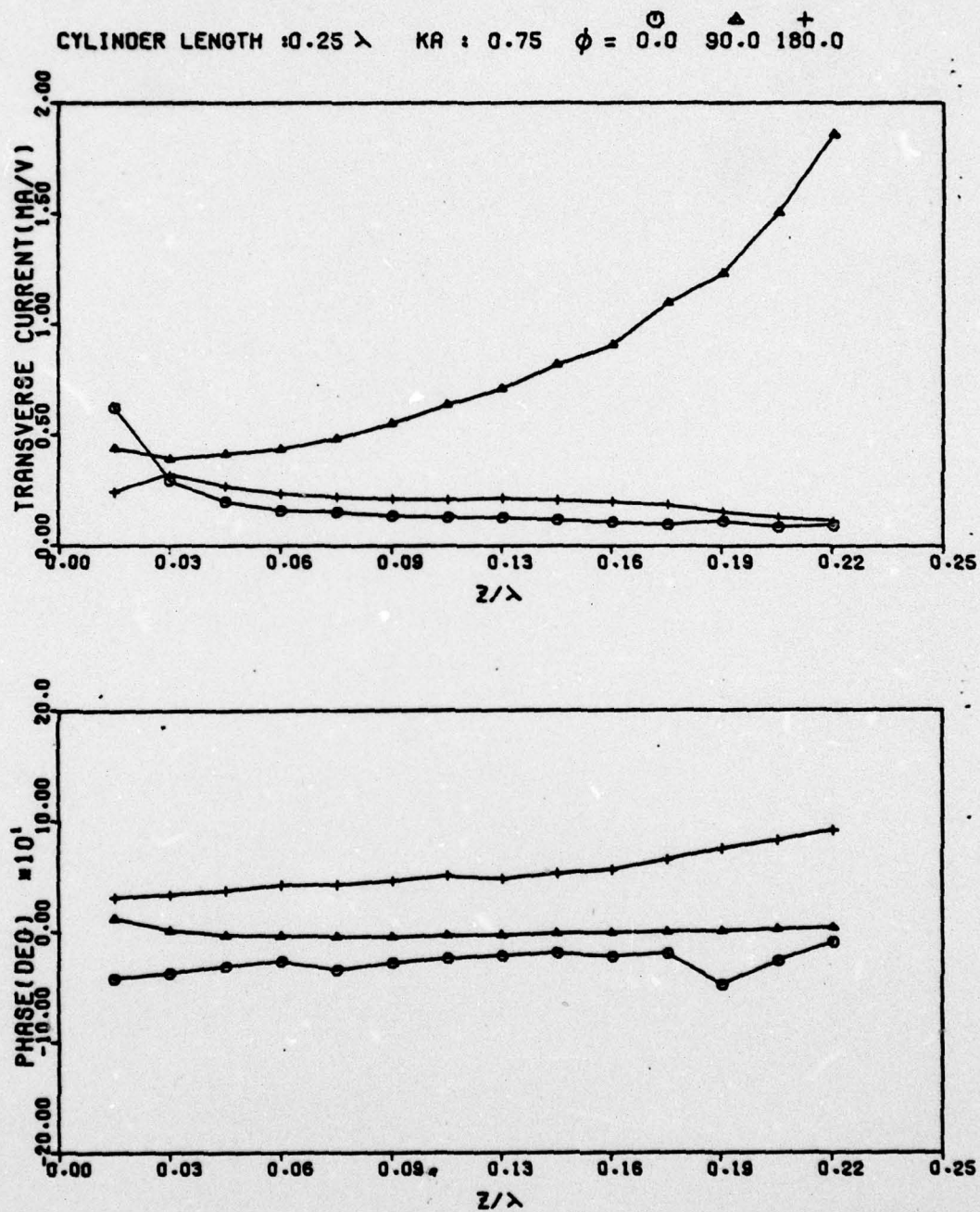


FIGURE 15 THICK CYLINDER TRANSVERSE CURRENT
 $h/\lambda = 0.25$ $ka = 0.75$

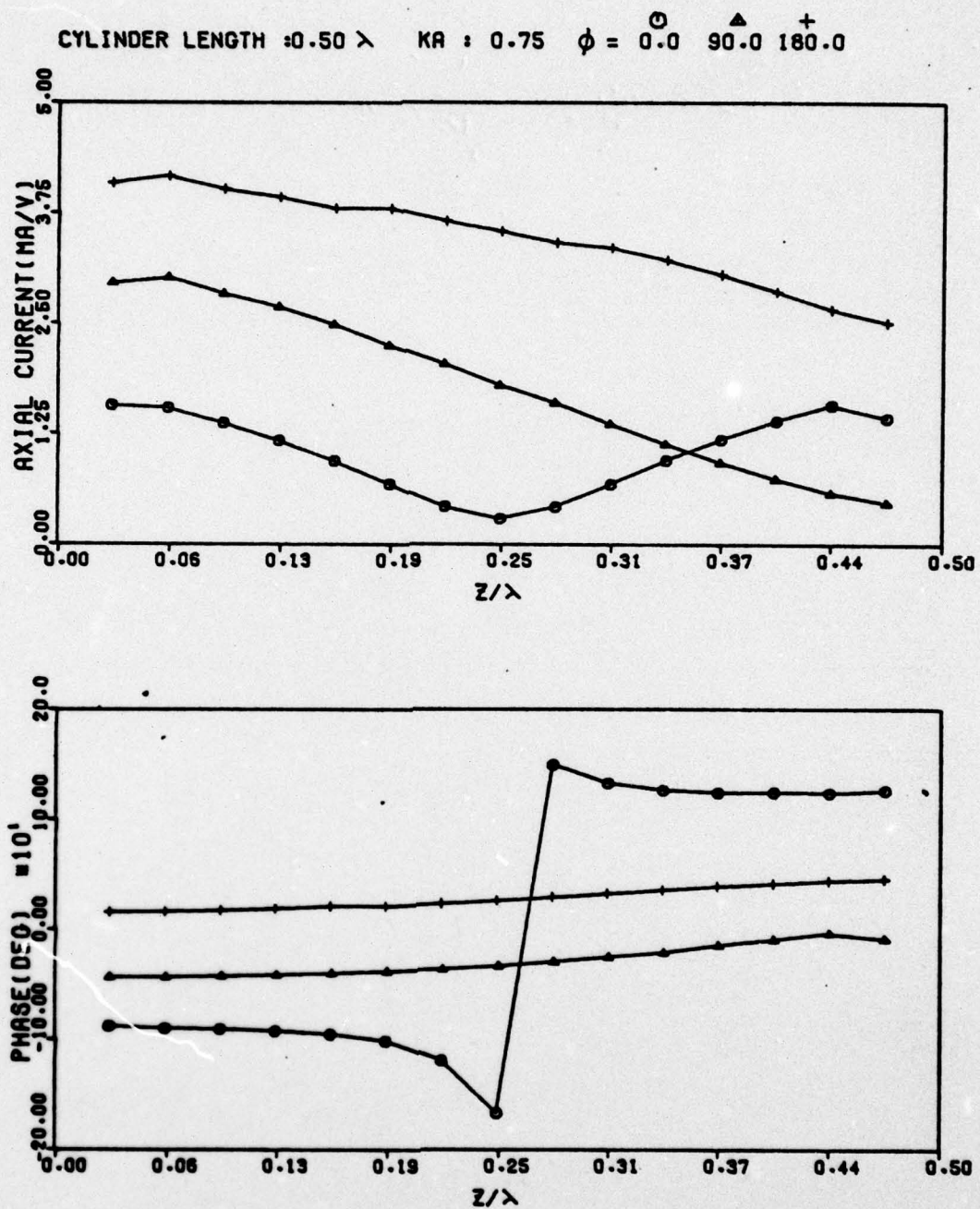


FIGURE 16 THICK CYLINDER AXIAL CURRENT
 $h/\lambda = 0.5$ $ka = 0.75$

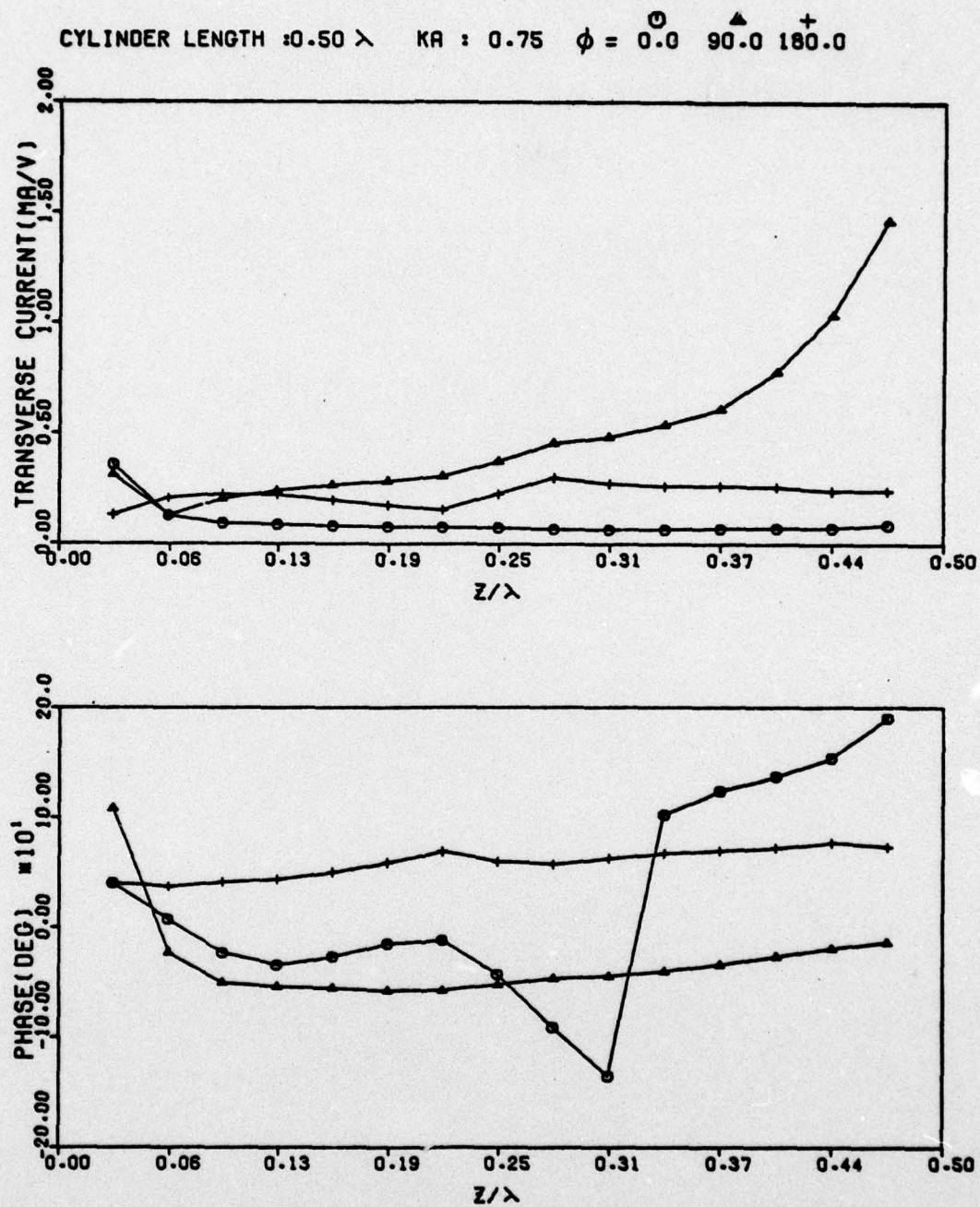


FIGURE 17 THICK CYLINDER TRANSVERSE CURRENT
 $h/\lambda = 0.5$ $ka = 0.75$

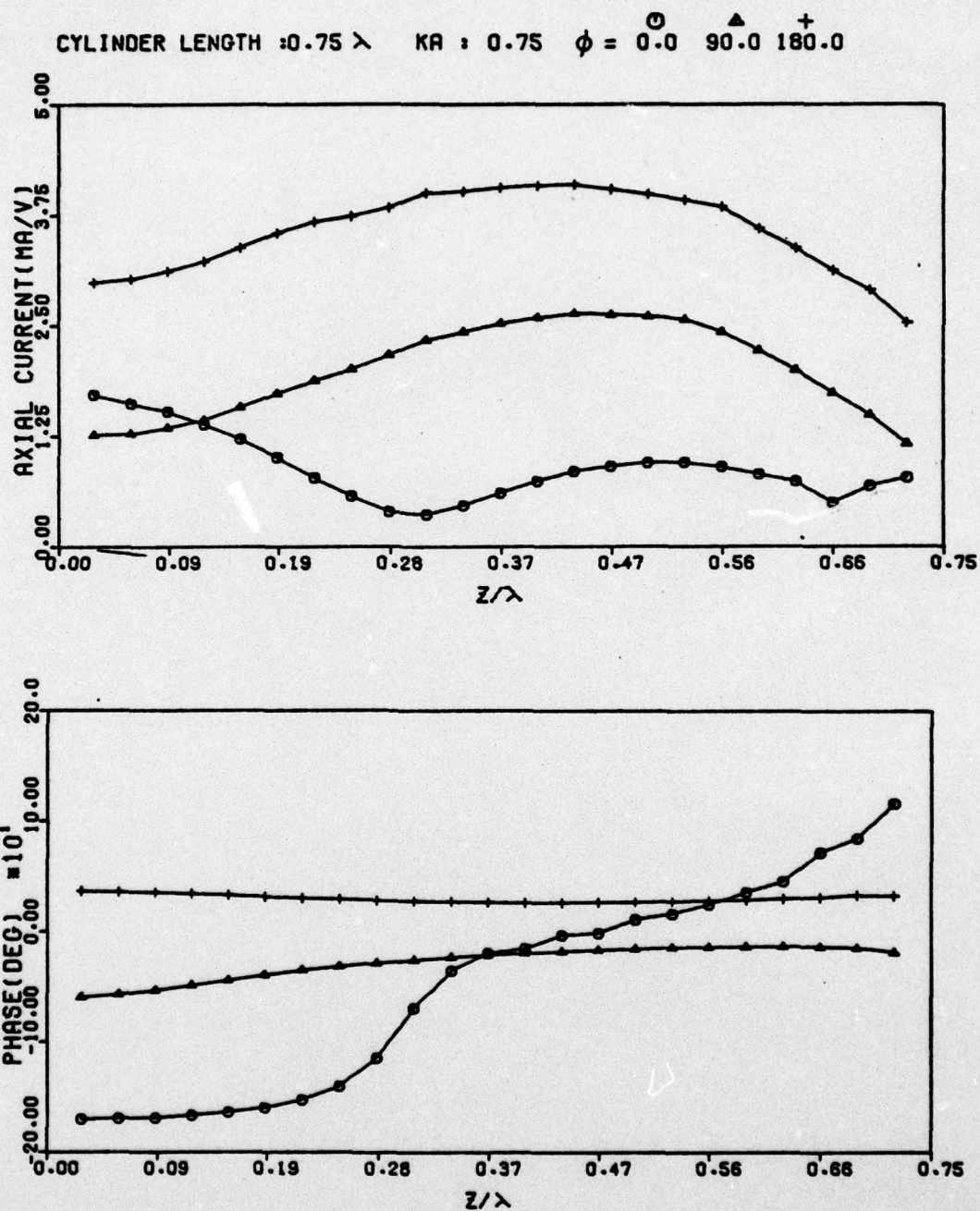


FIGURE 18 THICK CYLINDER AXIAL CURRENT
 $h/\lambda = 0.75$ $ka = 0.75$

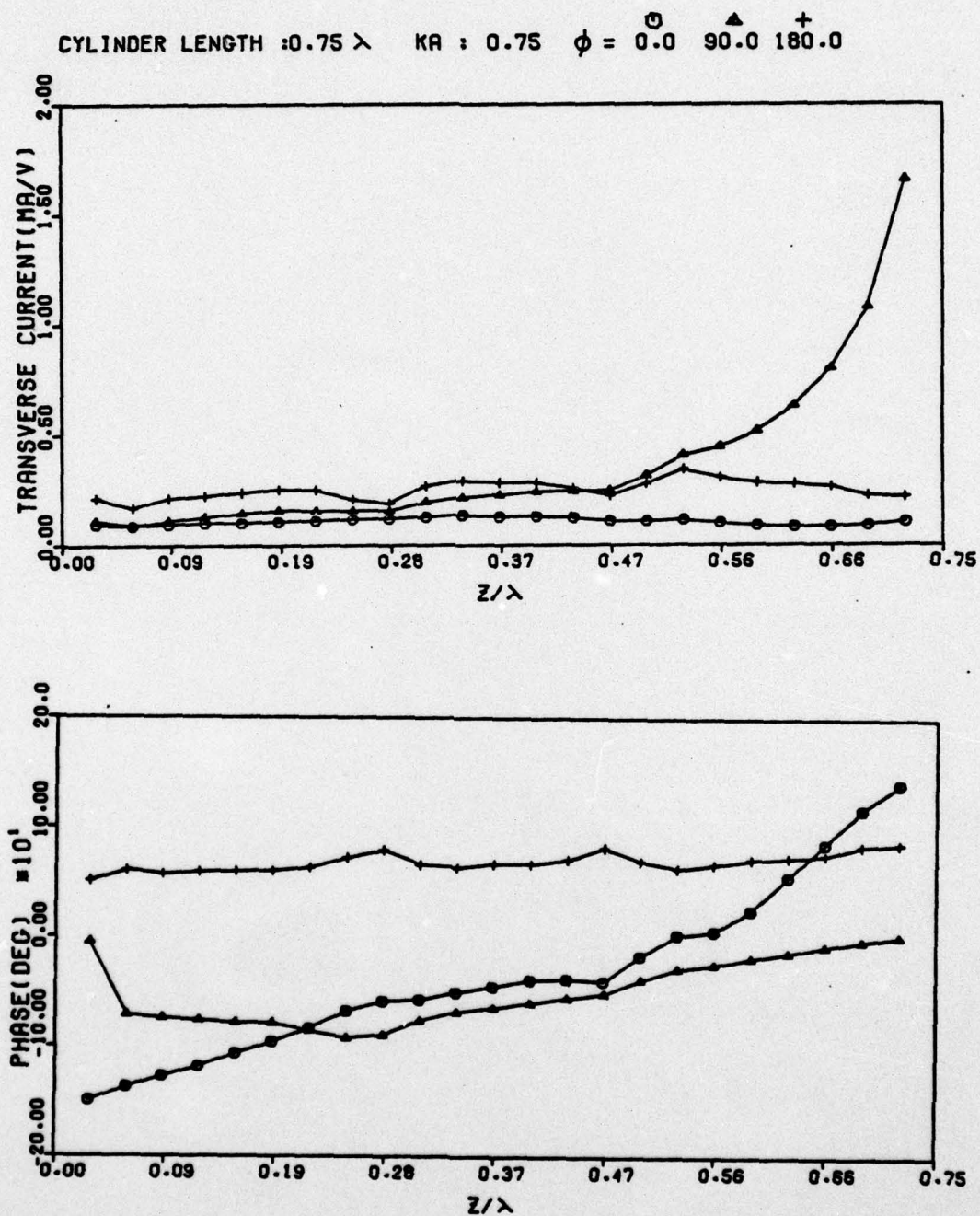


FIGURE 19 THICK CYLINDER TRANSVERSE CURRENT
 $h/\lambda = 0.75$ $ka = 0.75$

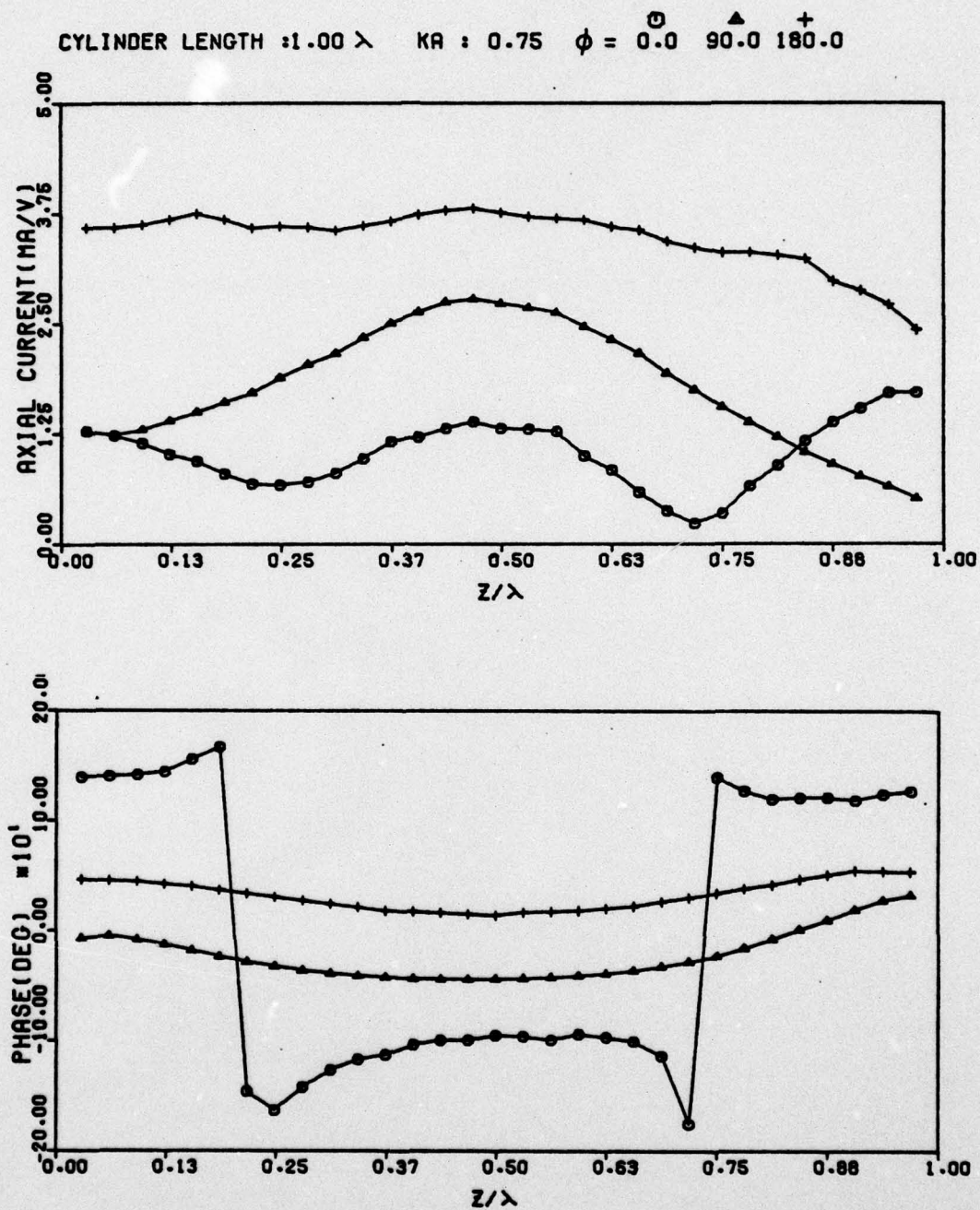


FIGURE 20 THICK CYLINDER AXIAL CURRENT
 $h/\lambda = 1.0$ $ka = 0.75$

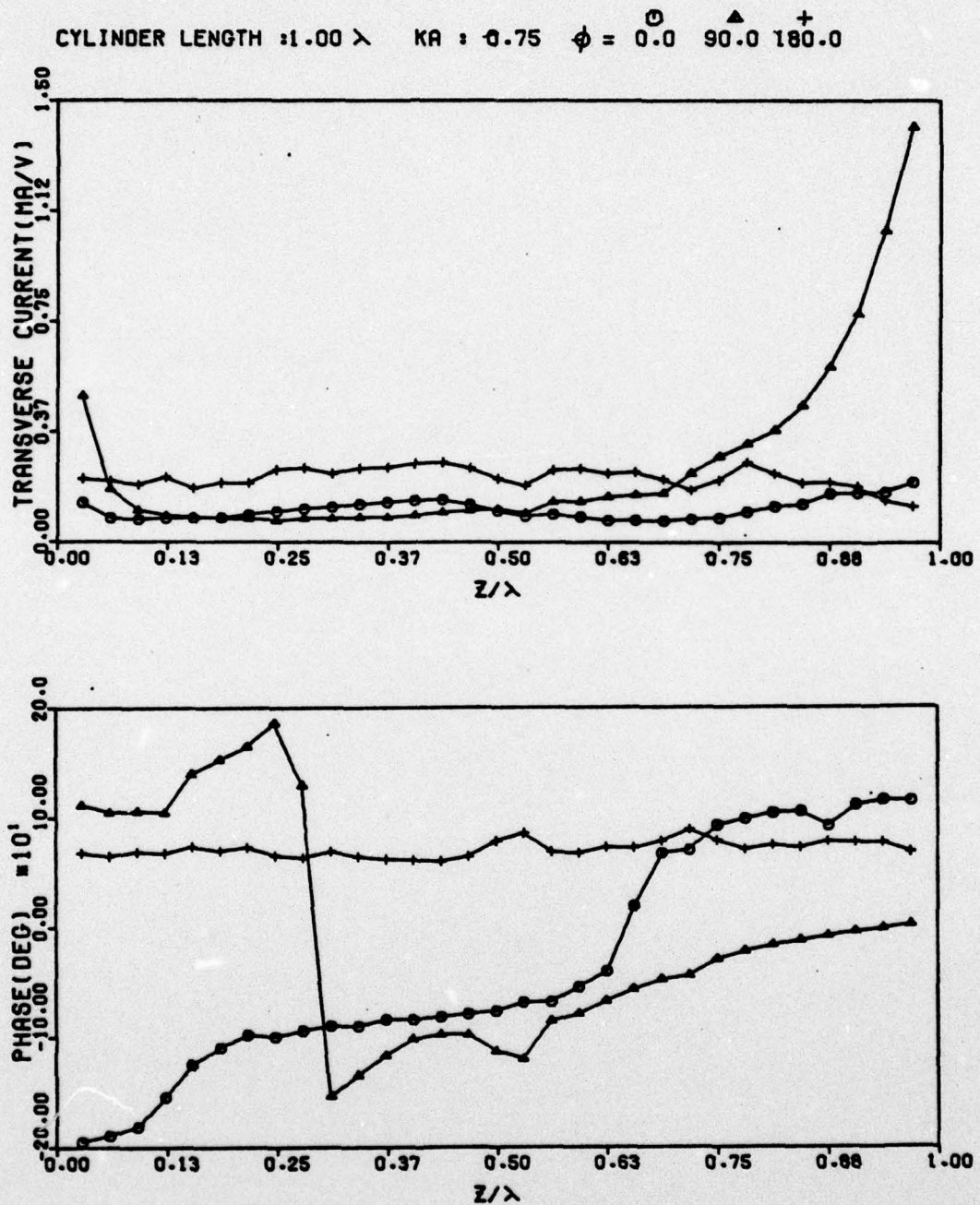


FIGURE 21 THICK CYLINDER TRANSVERSE CURRENT
 $h/\lambda = 1.0$ $ka = 0.75$

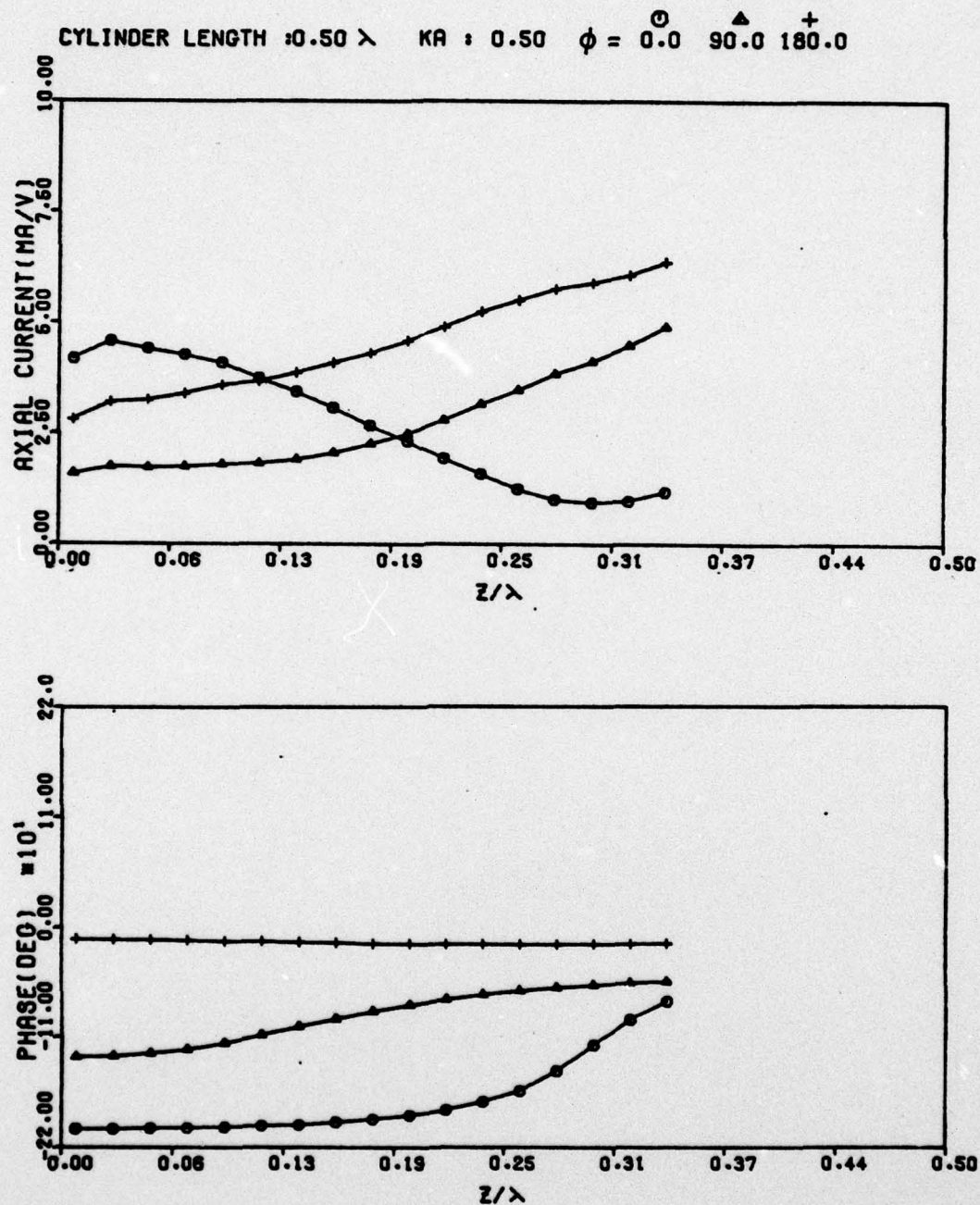


FIGURE 22 THICK CROSS AXIAL CURRENT ; GROUND PLANE TO JUNCTION
 $h_1/\lambda = 0.5$ $ka = 0.5$

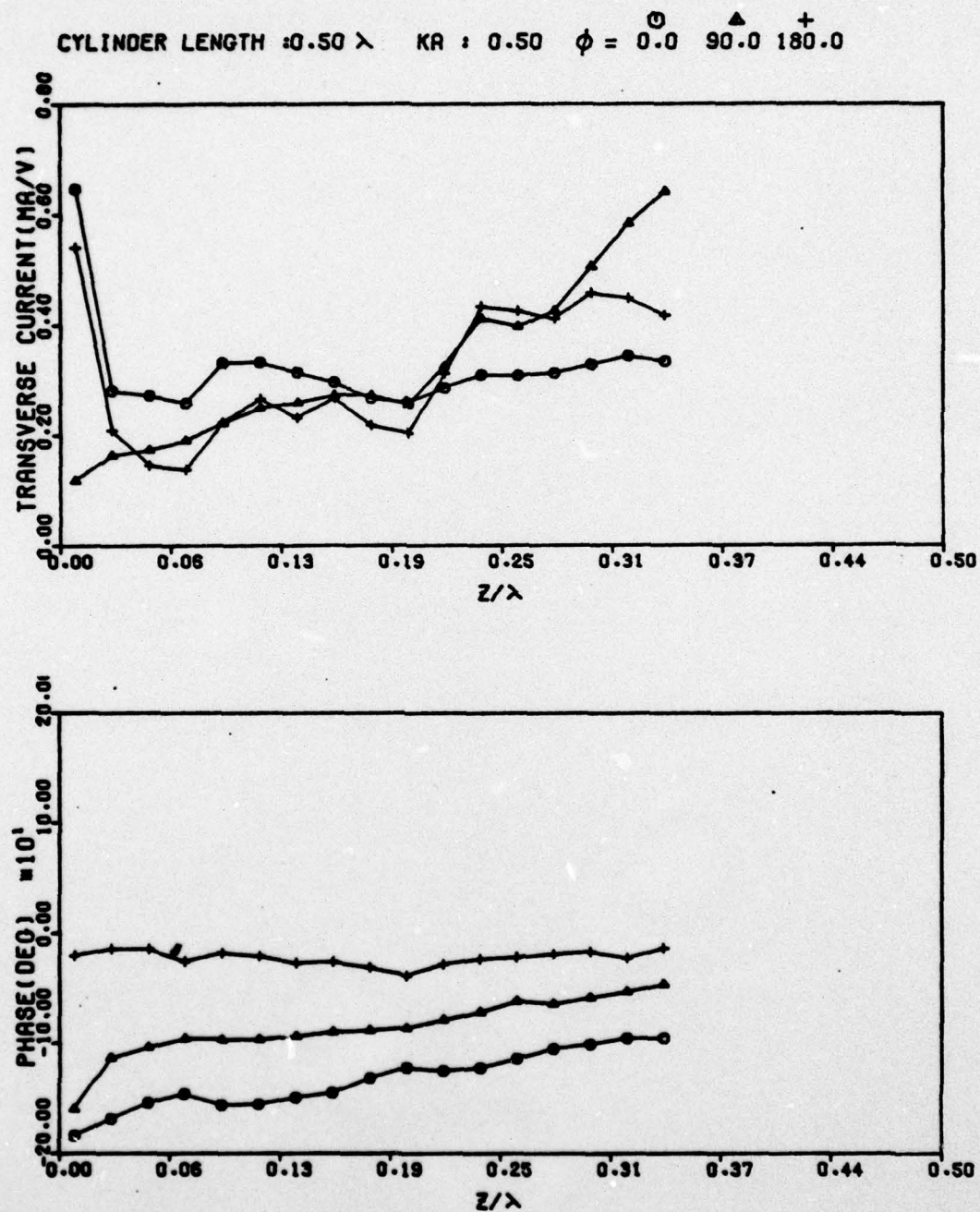


FIGURE 23 THICK CROSS TRANSVERSE CURRENT ; GROUND PLANE TO JUNCTION
 $h_1/\lambda = 0.5$ $ka = 0.5$

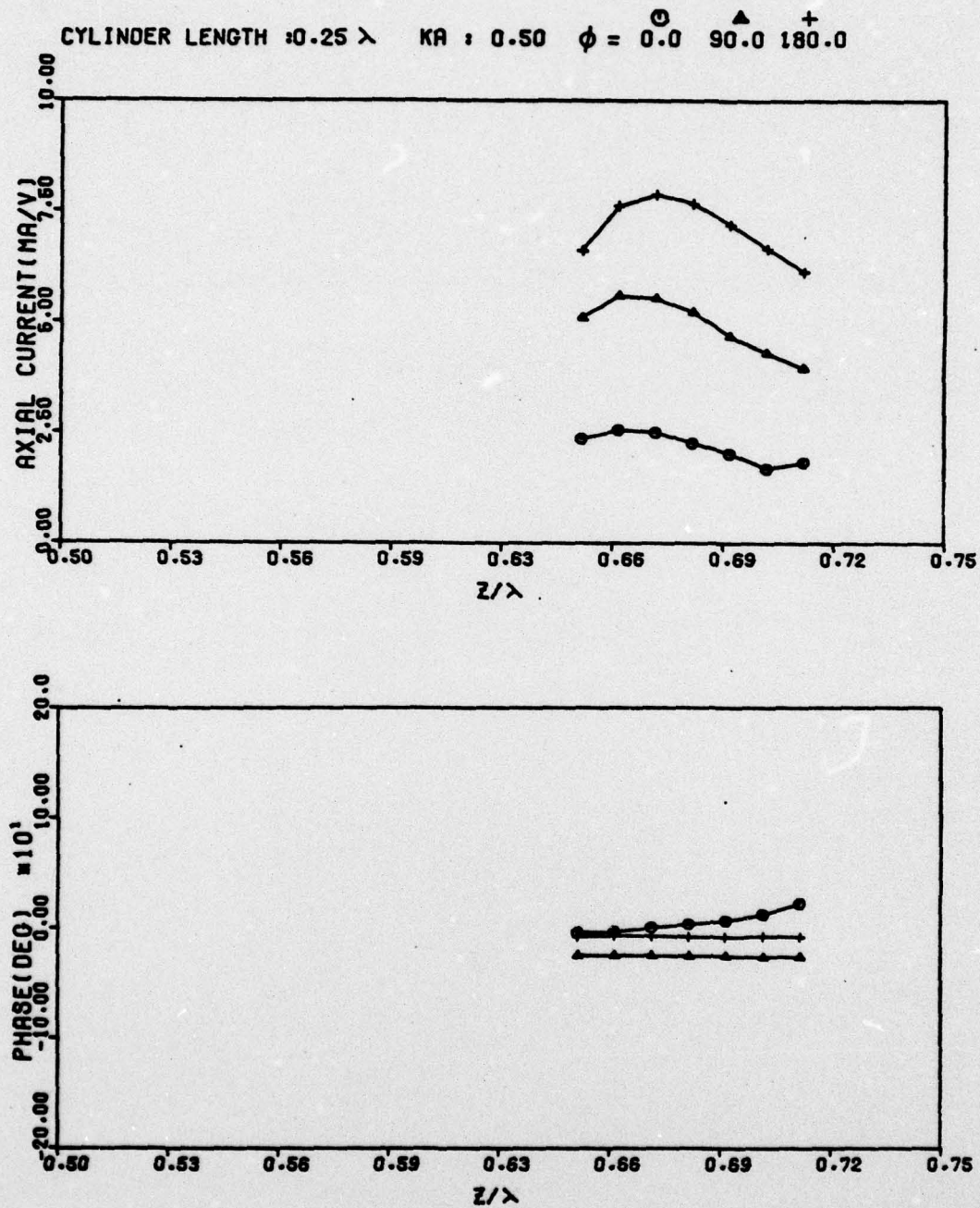


FIGURE 24 THICK CROSS AXIAL CURRENT ; JUNCTION TO END
 $h_2/\lambda = 0.25$ $ka = 0.5$

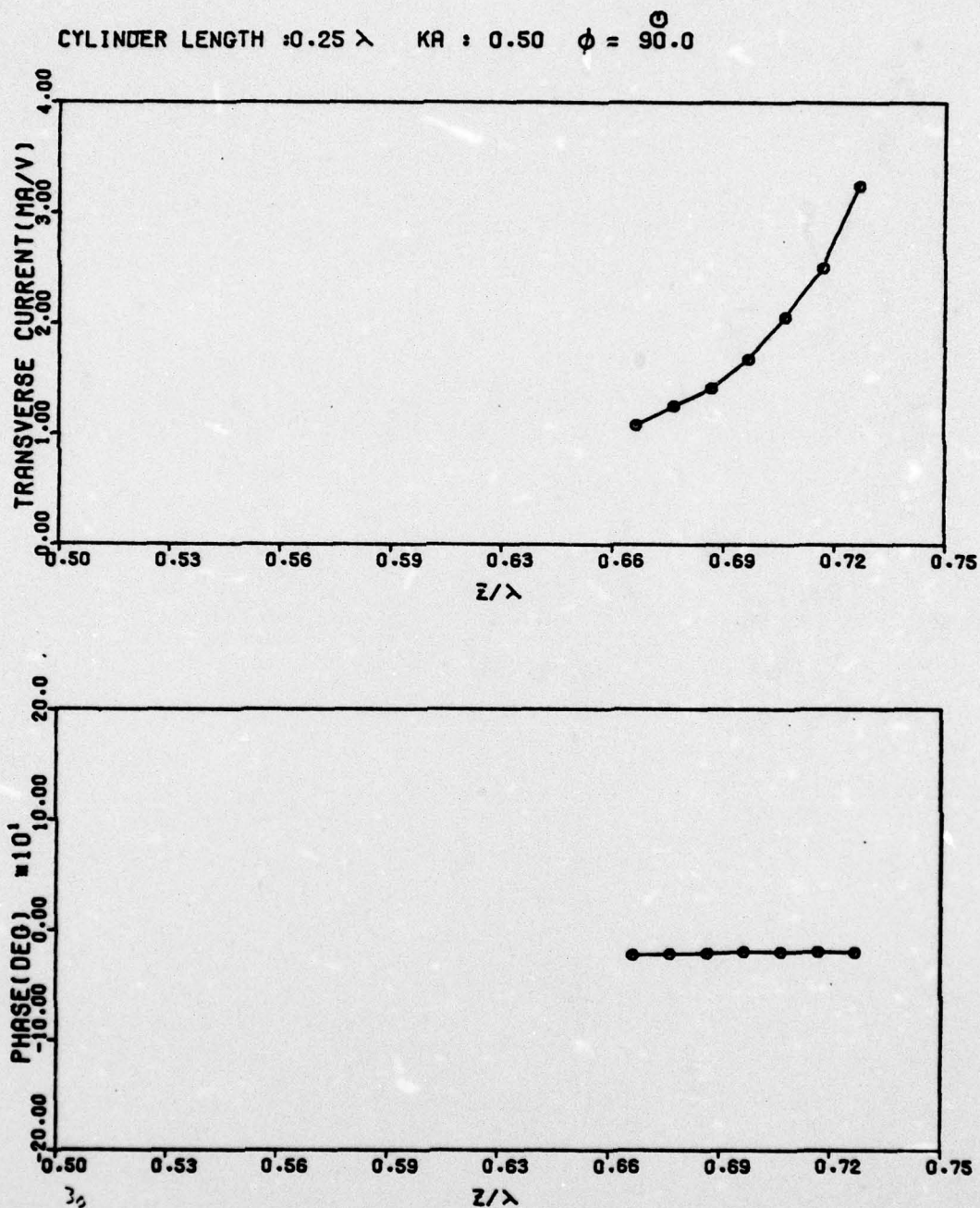
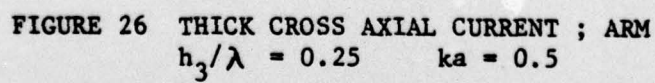


FIGURE 25 THICK CROSS TRANSVERSE CURRENT ; JUNCTION TO END
 $h_2/\lambda = 0.25$ $ka = 0.5$



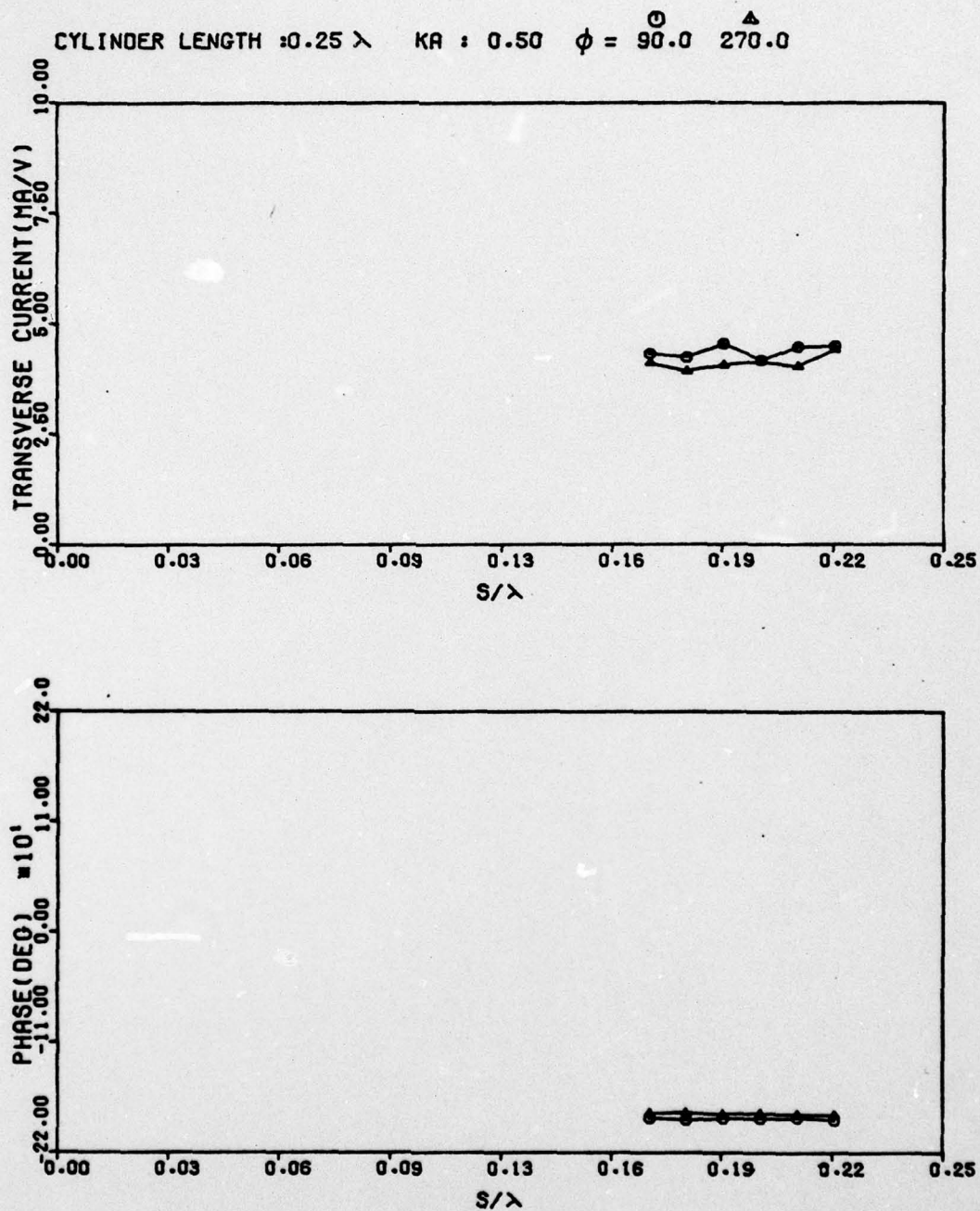


FIGURE 27 THICK CROSS TRANSVERSE CURRENT ; ARM
 $h_3/\lambda = 0.25$ $ka = 0.5$